DEUTSCHES ELEKTRONEN-SYNCHROTRON DESY

DESY 83-102
Oktober 1983

REVIEW OF e^+e^--PHYSICS WITH PETRA

by

E. Lohrmann

II. Institut für Experimentalphysik, Universität Hamburg

ISSN 0418-9833

NOTKESTRASSE 85 · 2 HAMBURG 52

To be sure that your preprints are promptly included in the
HIGH ENERGY PHYSICS INDEX ,
send them to the following address (if possible by air mail) :

DESY
Bibliothek
Notkestrasse 85
2 Hamburg 52
Germany

DESY 83-102
Oktober 1983

ISSN 0418-9833

Review of e^+e^--Physics with PETRA

E.Lohrmann *

II. Institut für Experimentalphysik, Universität Hamburg,

* Report based on a Talk given at the Topical Conference on Particle Physics at SLAC - 27-29 July 1983.

I. PARTICLE SEARCHES

Extensive searches for new particles have been undertaken in the past by the CELLO, JADE, MARK J, PLUTO and TASSO Collaborations. Their work is summarized in Review articles by A.Böhm[1], J.Bürger[2] and S.Yamada[3].

I shall not repeat these reviews here, but rather present an update by mentioning the most recent contributions.

1.1 Toponium

In its improvement program the PETRA e^+e^--storage ring has now (September 1983) been equipped with 112 RF cavities, and 9.6 MW of RF power have been installed. This allows a search for the top quark at the highest energies, which have so far been available in e^+e^--storage rings.

Production of $t\bar{t}$ bound states (toponium) occurs below the threshold for open top-quark production, and a scan for those states has been made. To this end the storage ring energy was moved upwards in steps of 30 MeV cms energy, and the experiments CELLO, JADE, MARK-J and TASSO measured the total hadronic cross section in a search for a toponium resonance. The size of the effect is given by

$$\int \sigma \cdot dE_{CM} = \frac{6\pi^2}{M^2} B_h \Gamma_{ee} \qquad (1)$$

where σ is the cross section for the production and subsequent hadronic decay of toponium, M is the toponium mass, B_h is the branching ratio of the toponium to decay into hadrons, Γ_{ee} is the toponium e^+e^--decay with, and E_{CM} is the CM energy.

Eq. (1) describes the area under the Breit-Wigner resonance curve of toponium. In the PETRA measurements the beam energy spread is about 24 MeV at a beam energy of 20 GeV, leading to a cms energy spread of about 34 MeV, and this is much larger than the natural width of toponium. One expects then to see a roughly Gaussian shape with σ ~34 MeV for the toponium signal, with the area still given by Eq. (1). In addition one has to take radiative corrections into account, which modify the shape of the signal appreciably.

Using $B_h \sim 0.8$ and $\Gamma_{ee} = 5$ keV, as expected for a quark of charge 2/3, the toponium signal should be easily visible under the conditions of the scan (see Fig. 1).

No signal has been observed up to a cms energy of 43.2 GeV. From the biggest fluctuations observed, all four experiments have obtained upper limits (95% c.l.) of about 2 keV [3] for $\Gamma_{ee} \cdot B_h$, which is well below the 4 keV expected for toponium.

The MARK-J experiment[4] has also put a limit on a possible step in the total hadronic cross section

$$\Delta R < 0.07 \qquad \text{for } 40 \text{ GeV} < E_{cm} < 43 \text{ GeV}$$

to be compared with the (asymptotic) step size of $\Delta R = 4/3$ after passing the threshold for open top quark production.

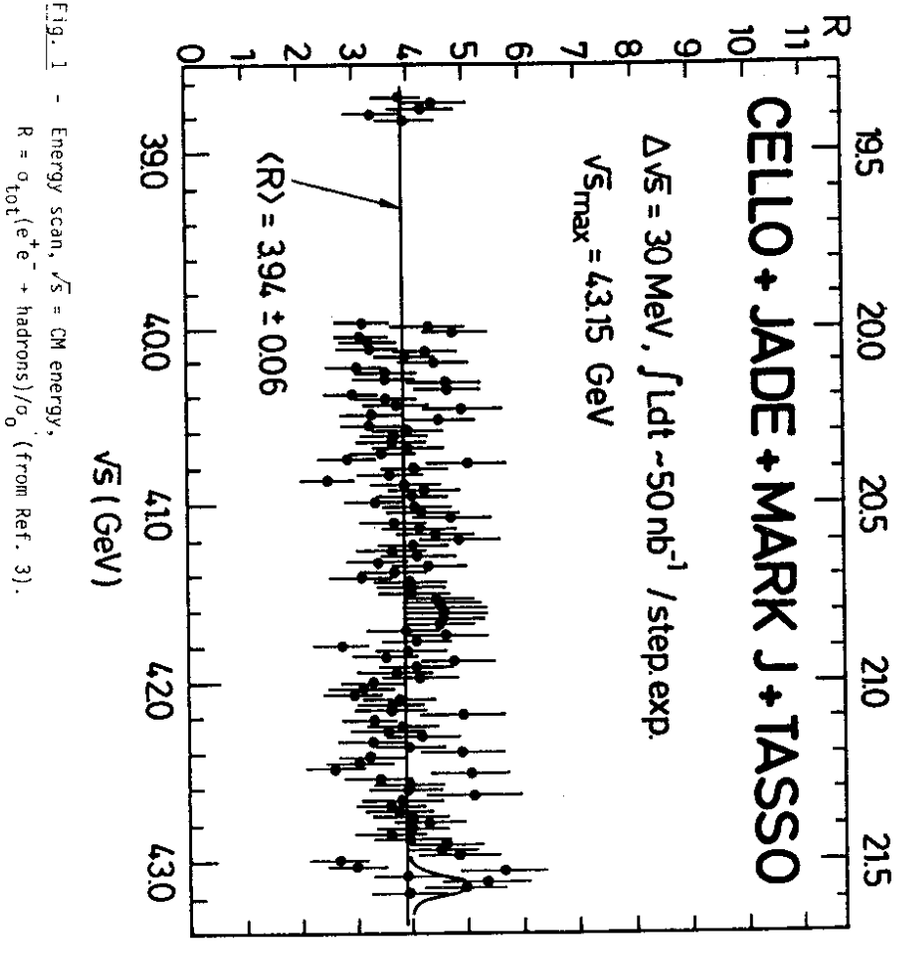

Fig. 1 - Energy scan, $\sqrt{s}$ = CM energy, $R = \sigma_{tot}(e^+e^- \to \text{hadrons})/\sigma_0$ (from Ref. 3).

1.2 Search for a b'-Quark

The MARK-J group and TASSO[5] have excluded the existence of a heavy b'-quark with charge $|Q| = 1/3$ for a mass M

$$M < 16 \text{ GeV}/c^2 .$$

The MARK-J group draws this conclusion from the dependence of the inclusive muon yield on the thrust T of the jets[4], and from the limit $\Delta R < 0.07$ mentioned above. Depending on assumptions on the threshold behavior, the mass limit may actually be higher.

1.3 Magnetic Monopole

A search for the production of magnetic monopoles was made with the help of Kapton foils placed inside the PETRA vacuum chamber. Monopoles would be detected in these foils by their high ionization rate. After exposure the foils are developed in 15% NaCl solution for 4 hours and any tracks would appear as holes in the plastic.

The charge g of a magnetic monopole is given by Dirac's equation

$$e \cdot g = n \cdot \frac{\hbar c}{2}$$

with n being an integer, n = 1, 2, 3, ...

The search was specifically made for monopoles with large magnetic charge $n > 1$. Fig. 2 shows the region of values n and monopole mass m excluded by the experiment [7]. It supplements earlier measurements made at SLAC[6]. Assuming a production process by monopole-antimonopole pair production $e^+e^- \to M\bar{M}$, an upper limit (95% c.l.)

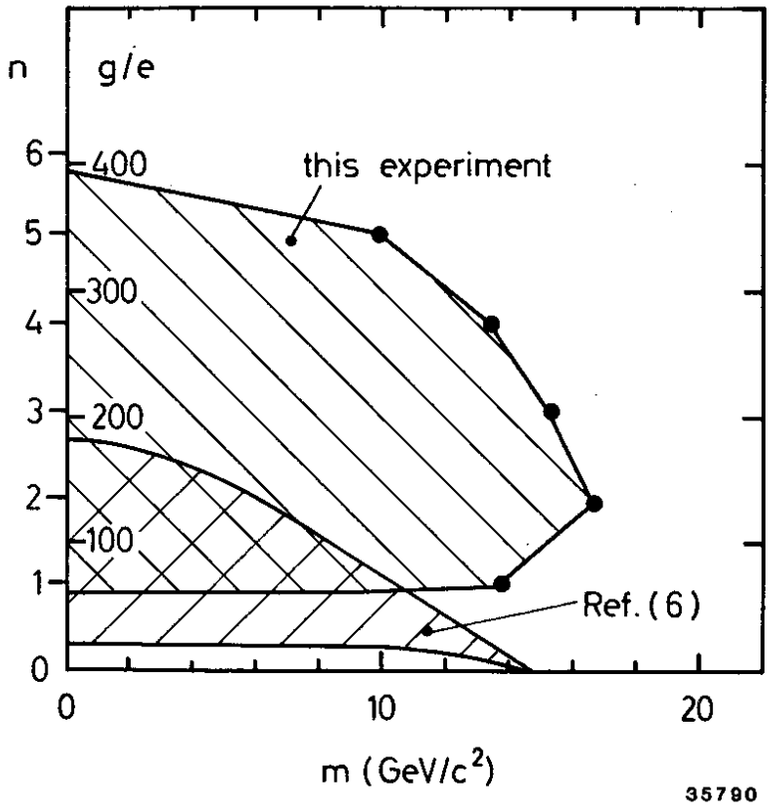

Fig. 2 - Monopole mass m, for which search is sensitive from Ref. 7); also shown is the result of Ref. 6.

on the cross section is

$$\sigma(e^+e^- \to M\bar{M}) \; < \; 4 \cdot 10^{-38} \text{ cm}^2 \; .$$

The corresponding R-value is

$$R_{M\bar{M}} = \sigma(M\bar{M}) \; / \; \sigma(\mu^+\mu^-) \; < \; 0.6 \cdot 10^{-3} \; .$$

1.4 Excited Leptons

Table 1.1 - Mass limits for excited leptons

	excluded mass
$e^* \to e\gamma$	$M < 61$ GeV
$\mu^* \to \mu\gamma$	$M < 17.9$ GeV

The mass limits in Table 1.1 are taken from the earlier review article by A.Böhm [1] and from new measurements by JADE [8].. They are derived from a study of $e^+e^- \to \gamma\gamma$ for e* (Fig. 3) and from a study of radiative corrections to $e^+e^- \to \mu^+\mu^-$ for the μ^*. The $e^*e\gamma$ ($\mu^*\mu\gamma$)-coupling is given by λe, the mass limits in Table 1.1 are derived for $\lambda = 1$.

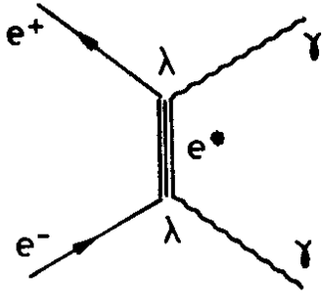

Fig. 3 - Hypothetical contribution to the QED reaction $e^+e^- \to \gamma\gamma$ by the exchange of an excited electron.

1.5 Sequential Lepton

A new lepton in the sequence e, μ, τ, ... would be detected by its decay into a muon or an electron and two neutrinos, the muon or electron appearing at large transverse momenta. A new limit has been set by the MARK-J [5] experiment and by JADE [8], excluding masses M:

$$M \; < \; 20.6 \text{ GeV} \quad \text{(JADE)} \; [8].$$

1.6 Heavy neutral Electron

A heavy neutral electron E^o would be coupled to the W-boson by the standard weak interaction, allowing V + A or V - A, see Fig. 4a.

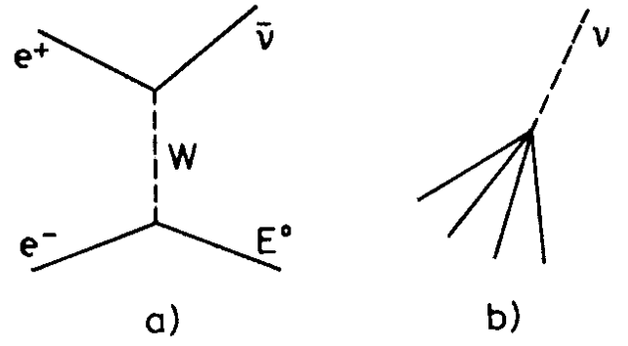

Fig. 4 - Production (a) and signature (b) of heavy neutral lepton E^o.

The E^o is produced via

$$e^+e^- \to E^o \bar{\nu}$$

with the E^o decaying via

$$E^0 \rightarrow e^- l^+ \nu_l, \; e^- \bar{d} u, \; e^- \bar{s} c$$

The JADE Collaboration[8] has searched for the E^0 by the signature shown in Fig. 4b, where one has a single jet from $e^- \bar{d} u$ going to one side. They can exclude an E^0 with a mass M

$$M < 23 \text{ GeV} .$$

1.7 Supersymmetric Particles

According to supersymmetry models[9], there is a pair of scalar particles corresponding to each spin 1/2 fermion and there is a supersymmetric fermion corresponding to each elementary scalar particle, see Table 1.2.

Table 1.2 - Supersymmetric Particles

Particle	supersym. partner (only one shown)	Decay
e electron	e_s	$e_s \rightarrow e \gamma_s$
μ muon	μ_s	$\mu_s \rightarrow \mu \gamma_s$
τ tau	τ_s	$\tau_s \rightarrow \tau \gamma_s$
q quark	q_s	$q_s \rightarrow g_s q, \; \gamma_s q$
γ photon	γ_s	$\gamma_s \rightarrow \gamma G_s^*$
g gluon	g_s	

* G_s = supersymmetric partner to the graviton; there may be other decays.

A review on mass limits for e_s, μ_s, τ_s achieved in earlier work has been given by A.Böhm [1]. The JADE Collaboration[8] has made a new search for e_s, μ_s, q_s and γ_s, where they consider the case of both stable and of unstable e_s and μ_s.

Production of a stable e_s or μ_s would look like $e^+e^- \rightarrow \mu^+\mu^-$, with a particle momentum of $P_s = \sqrt{E^2_{beam} - M^2}$; production of an unstable e_s or μ_s would lead to an e^+e^- or $\mu^+\mu^-$ pair with missing energy and momentum in the final state. The expected number of events of each type can be calculated from QED and a signal of the expected size can be excluded experimentally.

The search for q_s proceeds along similar lines. If the q_s is unstable, the unseen momentum carried away by the q_s would lead to two acoplanar quark-jets in the final state. From studying the measured acoplanarity distribution of jets the JADE Collaboration has derived mass limits[8] on the q_s but they had to choose specific assumptions on the decay of the q_s and on fragmentation.

The CELLO [10] Collaboration has made a search for a massive unstable γ_s. New data come from JADE [8].

Table 1.3 lists the mass values excluded by these searches.

Table 1.3 - Excluded Mass Values for Supersymmetry-Particles*

Particle	Mass excluded (GeV)	Remarks
e_s	$M < 16.6$	stable e_s
	$M < 17.8$	unstable e_s ($m_{\gamma_s}=0$)
μ_s	$M < 16.6$	stable μ_s
	$M < 18$	unstable μ_s (MARK-J)
τ_s	$M < 16.5$	MARK J
q_s	$2.5 < M < 13.5$	stable q_s
	$7.4 < M < 16$	unstable q_s, specific assumptions
γ_s	$M < 17$	if unstable, specific assumptions

*) See also Review of Particle Searches by A.Böhm [1].
Table 1.3 contains the most recent limits obtained by JADE, unless otherwise stated.

1.8 Charged Higgs /Technipion $H^{\pm}$

This scalar particle is coupled preferentially to heavy particles, so the dominant decay modes should be

$$H^+ \to \tau^+\nu_\tau, \to c\bar{s}, \to c\bar{b} .$$

Searches have been made by the CELLO, JADE, MARK J, MARK II, MAC and TASSO experiments[11]. In particular, the TASSO[12] experiment has excluded the case of predominant decay into heavy quarks. This excludes the following mass values for the H :

$$5 \text{ GeV} < M < 13 \text{ GeV} .$$

2. ELECTROWEAK AND WEAK INTERACTIONS

2.1 Cross Sections according to the Standard Model

Consider the differential cross section for the process: $e^+e^- \to f\bar{f}$ (f = fermion), described in lowest order by the Feynman diagrams of Fig. 5a).

$f \equiv e^-, \mu^-, \tau^-, q$.

$$d\sigma/d\Omega = \frac{\alpha^2}{4s} \left(R\,(1 + \cos^2\theta) + C\cos\theta \right. \qquad (2)$$

$$R = Q_f^2 - 2\, v_e v_f\, Q_f\, \mathrm{Re}(X) + (v_e^2 + a_e^2) \cdot (v_f^2 + a_f^2)|X|^2 \qquad (3)$$

$$C = -4\, a_e\, a_f\, Q_f\, \mathrm{Re}(X) + 8 v_e \cdot v_f\, a_e a_f |X|^2 \qquad (4)$$

(if f = quark, one must include a factor of 3 for color).

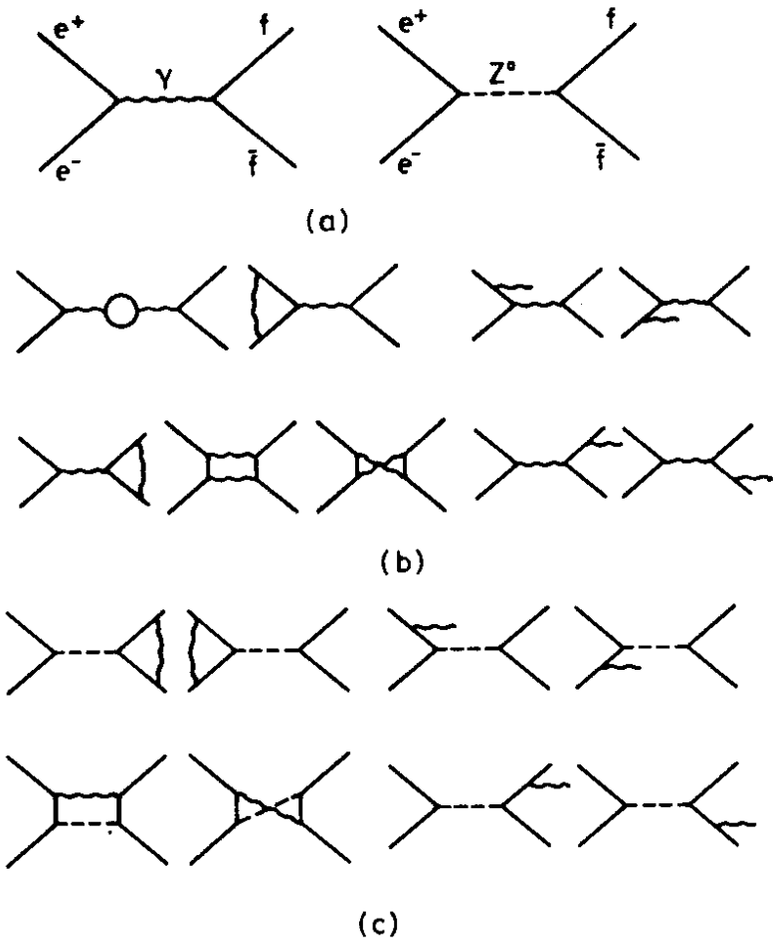

Fig. 5 - Feynman Diagrams for $e^+e^- \to f\bar{f}$ a) first order b) purely QED radiative corrections, c) radiative corrections including the Z^0 (additional weak radiative corrections not shown) b) included, c) not included in comparison of experiment and theory.

with

$$X = \frac{G_F}{2\pi\alpha\sqrt{2}} \cdot \frac{M_Z^2}{s - M_Z^2 + iM_Z\Gamma_Z}$$

Q_f = fermion charge, v_f, a_f are the weak vector and axial vector coupling constants, G_F (Fermi coupling constant) = $1.02 \cdot 10^{-10}/M_p^2$, M_Z = Z^0-mass. For the case of quarks one has to include QCD corrections, which are omitted here for simplicity, for the formulae, see Eq.(6)and Ref.(13).

The forward-backward asymmetry is given by

$$A_{ff} = \frac{F - B}{F + B} = \frac{3}{8}\frac{C}{R} \qquad (5)$$

where F = forward means the number of fermions going in the forward hemissphere as defined by the direction of the e^-, B = the same for backwards.

Table 2.1 gives the values of the coupling constants according to the standard model.

Table 2.1 - Coupling Constants according to the Standard Model

f	Q_f	a_f	v_f	v_f for $\sin^2\theta_W$=0.23
ν	0	1/2	1/2	1/2
e^-,μ^-,τ^-	-1	-1/2	$-1/2 + 2\sin^2\theta_W$	-0.04
u,c	2/3	1/2	$1/2-(4/3)\sin^2\theta_W$	0.19
d,s,b	-1/3	-1/2	$-1/2+(2/3)\sin^2\theta_W$	-0.35

where θ_W = Weinberg angle.

2.2 Lepton Asymmetry

New values for the muon asymmetry A have been given by JADE (-11.0 ± 1.8%), PLUTO (-12.4 ± 3.1%), MARK-J (-11.7 ± 1.7%) and TASSO (-9.1 ± 2.3%)[14]. These values include QED radiative corrections from diagrams containing only photons and electrons (Fig. 5b) and amounting to about +1.6% (slightly experiment dependent). The new weighted average at the average PETRA CMS energy of 34.5 GeV, including CELLO (-6.4 ± 6.4%) is

$$A_{\mu\mu} = (-10.9 \pm 1.0)\%$$

with an additional systematic error which I estimate to be 0.5%. This value can be compared with the prediction of the standard model Eq. (3,4,5), which for a Z^0-mass of 92 GeV and 34.5 GeV CM energy is

$$A_{\mu\mu}^{th} = (-9.3 \pm 0.3)\%$$

still in reasonable agreement with experiment.

Actually, for a comparison with the theoretical value of -9.3% the experimental value has in addition to be corrected for radiative effects from the diagrams containing a Z^0. The diagrams of Fig. 5c make an (experiment dependent) correction[15,16] which for TASSO (PLUTO) is 0.7% (+ 1.0%). Applying it would bring the TASSO (PLUTO) asymmetry to -9.8 ± 2.3% (-13.4 ± 3.1%). However, there are additional purely weak contributions to the radiative corrections (not shown in Fig. 5), whose size is not

yet clear. I have therefore preferred to omit the contributions from the diagrams in Fig. 5c.

The asymmetry for the tau lepton is[17]

$$A_{\mu\mu} = (-7.9 \pm 2.2)\%$$

again in agreement with the theoretical prediction.

The values of the muon and tau asymmetry $A_{\mu\mu}$ and $A_{\tau\tau}$ depend essentially on the three coupling constants a_e, a_μ, a_τ. In order to determine them separately from experiment, one needs a third experimental input, which one can take from measurements of neutrino-electron scattering. They yield[18]

$$a_e = -0.51 \pm 0.05 .$$

Using this value, one obtains then

$$a_\mu = -0.57 \pm 0.08$$

$$a_\tau = -0.42 \pm 0.11$$

to be compared with the standard-model value of -1/2. The combination of neutrino- and e^+e^--data allows in addition a resolution of the sign ambiguity of a_e and of the a_e/v_e ambiguity in the neutrino data [19], which has been used for the determination of a_e above.

These data provide a check of the standard model at four momentum transfers of $Q^2 = 1200\ \mathrm{GeV}^2$, and they are also an important check for e-μ-τ universality.

2.3 Heavy Quark Forward-Backward Asymmetry

Measuring this asymmetry provides an important check on the charges and the weak coupling of the heavy quarks. Experimentally one has to determine the flavor and the sign of the charge of the original quark, which is hidden in the jets.

Two methods have been used:

i) $e^+e^- \rightarrow c\,\bar{c} \rightarrow D^{*+}\,D^{*-}$

It has been possible to identify the D* experimentally[20]. Since the D*'s have a hard momentum spectrum (average momentum ≈ 60% of the beam energy), one believes that the D^{*+} follows the direction of the c-quark.

ii) $e^+e^- \rightarrow c\,\bar{c}$, $c \rightarrow s\,W^+$, $W^+ \rightarrow l^+\,\nu_l$

$\rightarrow b\,\bar{b}$, $b \rightarrow c\,W^-$, $W^- \rightarrow l^-\,\bar{\nu}_l$

In this method one uses the semileptonic ($l^\pm = e^\pm$ or $\mu^\pm$) D- and B-decays to tag the c- and b quarks. The method has its difficulties, because one can only achieve a partial separation of leptons coming from c- and b-decay, and because of a background of misidentified leptons.

Fig. 6 gives as an example the inclusive muon transverse momentum spectrum as obtained by MARK-J. The figure also shows the muon spectra expected from semileptonic c- and b-decay separately and one sees how they add up to give the measured curve. By choosing appropriate cuts in transverse momentum, momentum and maybe other variables of the jets, one tries to get data samples enriched in c- or b-decay events, and then uses them to compute the asymmetry. This still requires a critical subtraction of background.

Table 2.2 gives a summary of results.

The values are in accord with the standard model!

2.3 Vector Coupling Constant

At PETRA energies the weak vector coupling constants v_f appear essentially in the expression for the total cross sections. Table 2.1 shows, that one has small numerical values of v_f in the standard model. Accordingly the effects of weak interactions are at the limit of observability. Still this can serve to set upper limits on the v_f-coupling constants and therefore limits on $\sin^2\theta_W$.

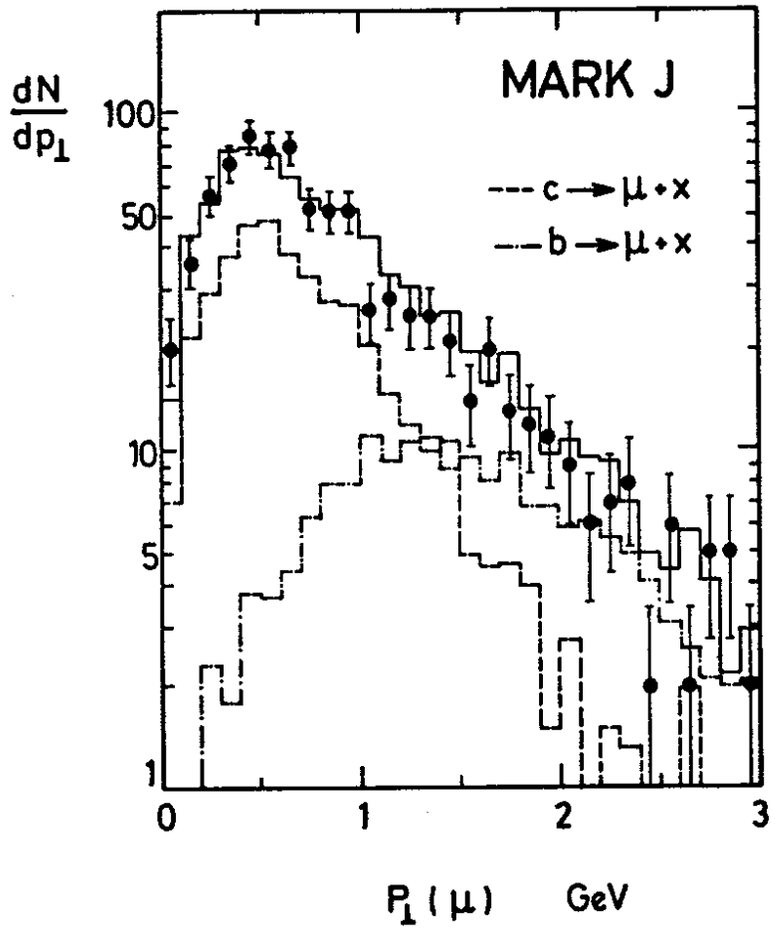

Fig. 6 - Distribution of inclusive muon transverse momentum relative to the jet axis, also shown are predicted contributions from semileptonic c- and b-decays. The solid histogram is the prediction with u,d,s,c and b quarks including decay and punchthrough.(Ref. 4).

Table 2.2 - Forward-Backward Asymmetry of Heavy Quarks [21]

	$A_{c\bar{c}}$	$A_{b\bar{b}}$	Method
TASSO	-0.13 ± 0.10		$D^*\bar{D}^*$
TASSO		-0.38 ± 0.28	μ incl.
JADE	-0.27 ± 0.14		$D^*\bar{D}^*$
JADE		-0.26 ± 0.09	μ incl.
MARK-J	-0.17 ± 0.09	-0.15 ± 0.22	μ incl.
average	-0.17 ± 0.06	-0.25 ± 0.08	
standard model prediction	-0.14	-0.25	

From a new accurate measurement of the total hadronic cross-section (see section 3.1) the JADE Collaboration obtains

$$\sin^2\theta_W = 0.23 \pm 0.05 .$$

From an overall fit to the leptonic reactions $e^+e^- \to e^+e^-$ and $e^+e^- \to \mu^+\mu^-$ the TASSO Collaboration gets[14]

$$\sin^2\theta_W = 0.26 \pm 0.07 .$$

These values agree with the world average of 0.23. The errors are larger than those achieved by neutrino experiments or by experiments with polarized e- or μ-beams. Still the results are interesting, because the measurement has been done at the very large value of $Q^2 \approx 1200\ \text{GeV}^2$.

2.4 Branching Ratios for τ- and heavy Quark Decay

The CELLO Collaboration has communicated new measurements of branching ratios of tau decay. The results are[22]

$$BR(\tau \to \rho\nu) = (22.8 \pm 2.5 \pm 2.1)\%$$
$$\to \pi\nu) = (9.9 \pm 1.7 \pm 1.3)\%$$
$$\to e\nu\nu) = (18.3 \pm 2.4 \pm 1.9)\%$$
$$\to \mu\nu\nu) = (17.6 \pm 2.6 \pm 2.1)\%$$

The branching ratios for the semileptonic decays of c- and b-quarks can be obtained from the inclusive electron or muon momentum spectra. First one has to separate the contributions from c-decay, b-decay and background in the spectra, as explained in section 2.2.

If one then assumes, that the numbers of hadrons containing a $(\bar{c})$- or $(\bar{b})$-quark are respectively 2 x (4/11) or 2 x (1/11) per event, one obtains the semileptonic branching ratios of Table 2.3.

Table 2.3 - Semileptonic Branching Ratios of Hadrons containing c- and b-quarks[23]

Experiment	c μ X (%)	b e X (%)	b μ X (%)
CELLO	12.3 ± 2.9 ± 3.9	14.1 ± 5.8 ± 3.0	8.8 ± 3.4 ± 3.5
MARK J	11.5 ± 1.0 ± 1.7	-	10.5 ± 1.5 ± 1.3
TASSO	-	13.6 ± 4.9 ± 4.0	15.0 ± 3.5 ± 3.5
Average	11.6 ± 1.0 ± 1.7	13.9 ± 3.8 ± 2.5	10.8 ± 1.3 ± 1.1

Upper limits of 0.7% have been found for the branching ratio of $b \to \mu^+\mu^- X$ by the JADE and MARK J Collaboration[24]. This limit excludes certain models[25] having 5 quark flavors instead of 6.

3. STRONG INTERACTIONS

3.1 Measurement of α_s

The JADE Collaboration has made a new accurate measurement of the total hadronic cross section (see Fig. 7) and improved earlier[26] measurements by TASSO ($R = 4.01 \pm 0.03 \pm 0.2$) and MARK-J ($R = 3.84 \pm 0.05 \pm 0.22$). (See also MAC ($R = 3.89 \pm 0.02 \pm 0.11$)).

The average R- value of JADE[26] is

$$\langle R \rangle = \frac{\sigma_T(e^+e^- \to \text{hadrons})}{\sigma_0(e^+e^- \to \mu^+\mu^-)} = 3.97 \pm 0.05 \pm 0.10$$

where $\sigma_0 = \frac{4\pi}{3}\alpha^2/s$ and $s = E_{CM}^2$.

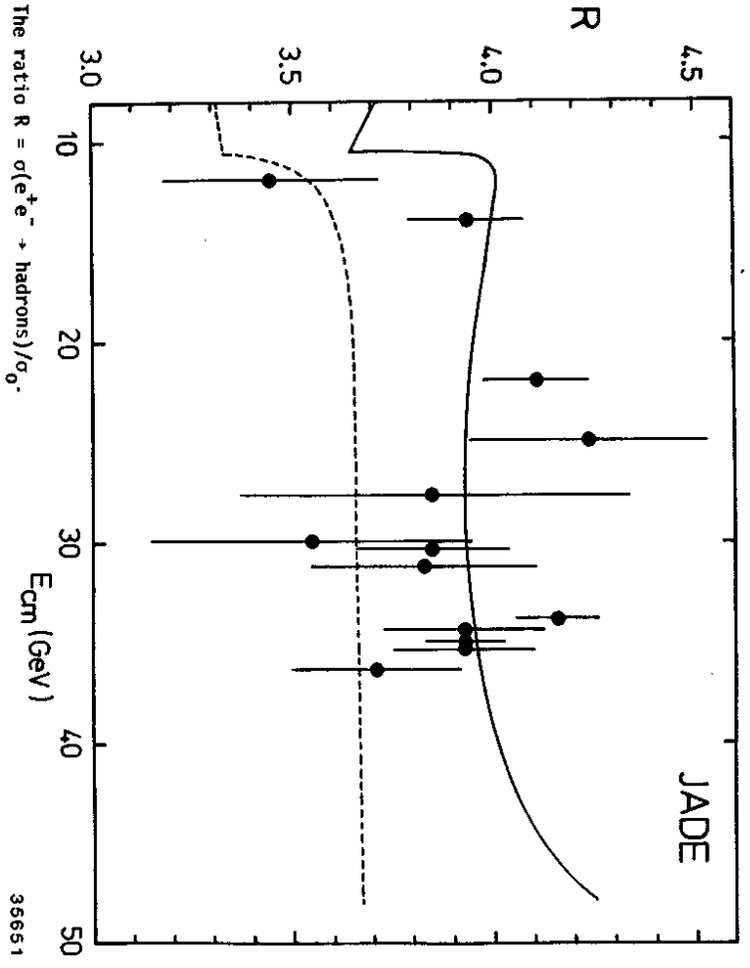

Fig. 7 - The ratio $R = \sigma(e^+e^- \to \text{hadrons})/\sigma_0$. Dashed curve: quark parton model; full curve: fit to Eq.6, plus weak interaction corrections.

The theoretical expression for R, including QCD, but without weak interaction corrections, is ($\overline{MS}$ scheme, 5 flavors)

$$R = 3\cdot(1 + \frac{\alpha_s}{\pi} + C_2(\frac{\alpha_s}{\pi})^2)\cdot\sum_q Q_q^2 \qquad (6)$$

$$C_2 = 1.99 - 0.12\ N_f = 1.39)$$

(with a factor 3 for color included; for the full formula including weak interaction corrections, see Ref.26).

From a simultaneous fit to the strong coupling constant α_s and to $\sin^2\theta_W$ they obtain

$$\alpha_s = 0.20 \pm 0.08 \quad \text{and}$$
$$\sin^2\theta_W = 0.23 \pm 0.05 \quad \text{(see 2.3)}\ .$$

This method of finding α_s is on a sound theoretical basis, but the experimental errors are large, because R depends on α_s roughly as

$$R \approx 3\Sigma\ Q_f^2\ (\ 1 + \frac{\alpha_s}{\pi})$$

α_s being contained in the correction term.

In contrast the relative frequency of three-jet events arising from gluon bremsstrahlung (see Fig. 8b) should depend on α_s directly and therefore allow a potentially more acurate determination of α_s.

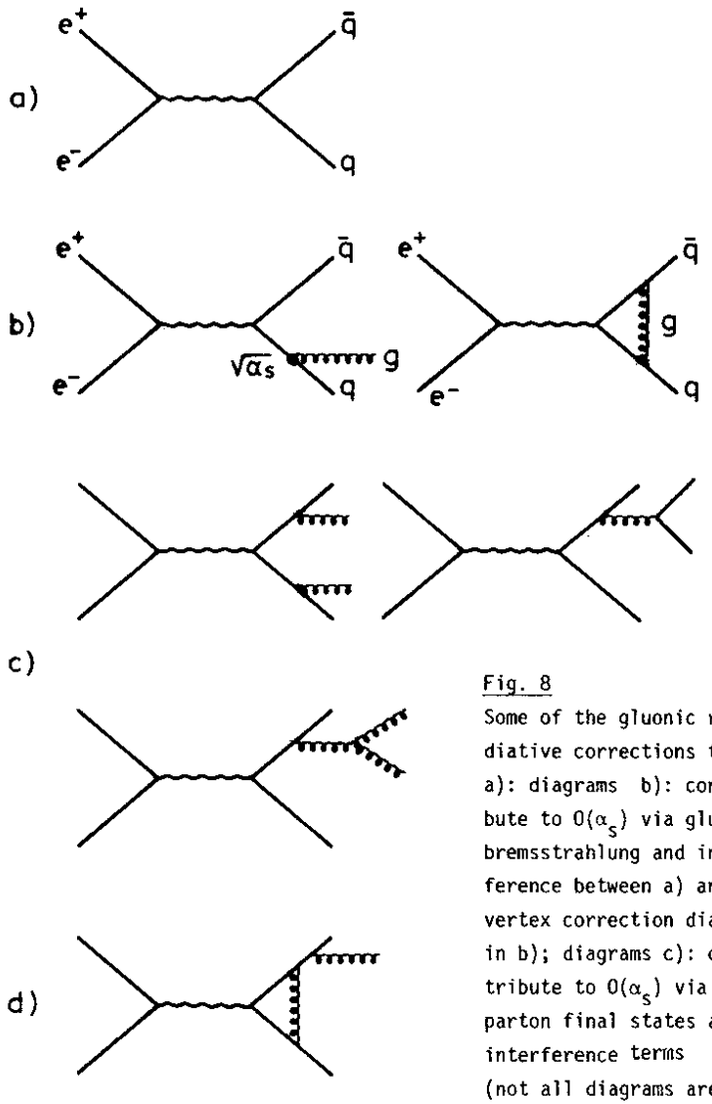

Fig. 8
Some of the gluonic radiative corrections to a): diagrams b): contribute to $O(\alpha_s)$ via gluon bremsstrahlung and interference between a) and vertex correction diagram in b); diagrams c): contribute to $O(\alpha_s)$ via four parton final states and interference terms (not all diagrams are drawn).

However, there are now other difficulties. Firstly, there are the higher order corrections Fig. 8c - 8d). Although the various theoretical results on the next higher order $O(\alpha_s)^2$ now roughly agree and we understand how one has to choose the cuts on the experimental data in the correct way[27], there may still be small but important differences [28].

The corrections are not large enough to raise wories on the validity of the perturbation series, but still large enough to matter. Indeed, all PETRA groups have now results derived from comparison with QCD calculations in $O(\alpha_s)^2$.

We now come to the second difficulty. The QCD calculations in perturbation theory are valid on the level of the partons, the quarks and gluons. The observation however is in terms of jets of hadrons. In order to go from jets to partons, one needs phenomenological models on the hadronization process of the partons. Two extreme models are shown in Fig. 9, the independent fragmentation model à la Feynman Field (IP) and the string model à la Lund (LD).

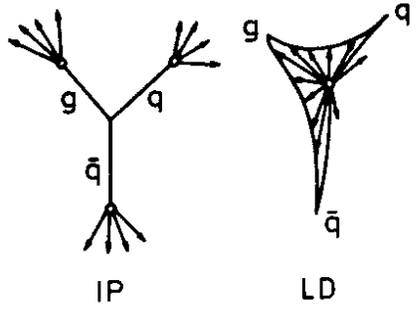

Fig. 9 - Hadronization via the independent parton model (IP) (each parton fragments into hadrons) and the string model (LD): hadronization along color flux lines stretched between gluon and quarks.

The PETRA groups have invested a great amount of work to fit the two models to the data and to compare to second order QCD calculations. The result is shown in Fig. 10.

The CELLO Collaboration has used the asymmetry of the energy-energy correlation[29]. This method is unfortunately - contrary to earlier hopes - also sensitive to fragmentations. In addition, it appears to be sensitive to the way energy conservation is introduced into the fragmentation models. The independent parton model (IP) and the string model (LD) give different results. This sensitivity to fragmentation had already been pointed out by earlier work of CELLO[30].

The JADE Collaboration used cluster analysis to reconstruct the original partons, and used the distribution of x_{max} (x-value of most energetic parton) and $x_\perp$ (transverse x of other parton). They find - within errors - no dependence on the fragmentation model[31].

MARK-J used the asymmetry of the energy-energy correlation[32].

TASSO fitted a number of event shape parameters to the data in both models, and got good agreement between the data and the model predictions for the listed values of α_s. Like CELLO, they see an appreciable dependence on the fragmentation model.

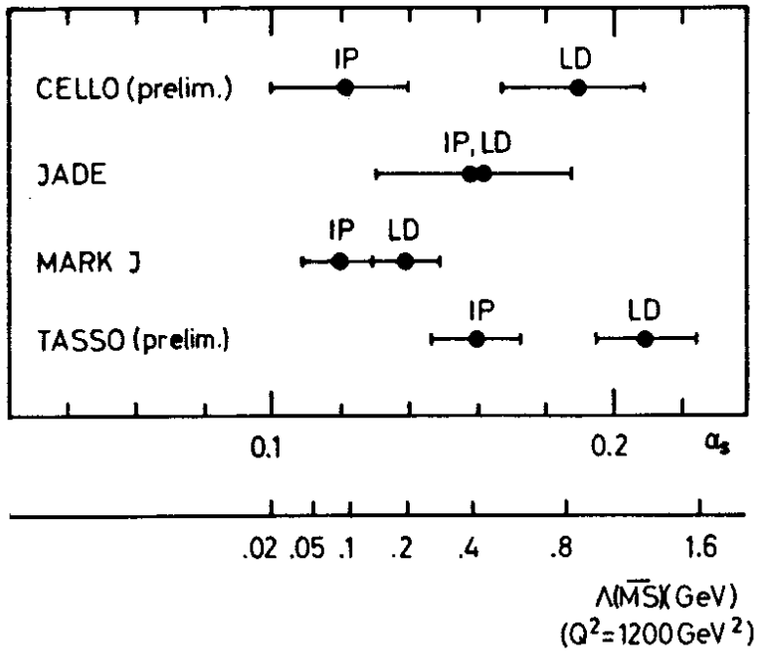

Fig. 10 - Measurement of α_s in second order by PETRA groups;
IP = independent parton model,
LD = string model used for fragmentation.

The groups differ in the way they apply second order corrections. MARK-J has used the work of ERT[34], the other three groups have used FKSS[35]. This could also be a source of disagreement.

In summary the Lund model gives larger values of α_s than the IP-model, but there is disagreement on the size of this effect. It also appears that the value of α_s obtained in the analysis is sensitive to the way the second order corrections are applied. Since the IP and LD models constitute two extremes among fragmentation models, I believe that the true value of α_s may lie between $\alpha_s = 0.12$ and $\alpha_s = 0.22$. Whereas one could imagine worse measuremets of α_s, it is not accurate enough to yield a useful value*) for $\Lambda_{\overline{MS}}$. Obviously one needs more information to make progress, such as, e.g., the energy dependence of jet measures, as first tried by the PLUTO Collaboration[36]; and maybe a new look at second order corrections.

3.2 General Properties of the Hadronic Final State

i) The PLUTO Collaboration has presented interesting studies on the transverse momentum of jets and on energy moments à la Konishi, Ukawa and Veneziano[37].

---

*) In second order, and in the $\overline{MS}$ renormalisation scheme

$$\alpha_{s,\overline{MS}}^{(2)} = \frac{12\pi}{(33-2N_f)\ln(s/\Lambda^2) + \frac{6\cdot(153-19N_f)}{(33-2N_f)} \cdot \ln\ln(s/\Lambda^2)}$$

where N_f = number of flavors = 5, s = (cm energy)^2.

ii) The JADE Collaboration[38] has presented new measurements of the mean number of charged particles in a jet $\langle n_s \rangle$ as a function of cm energy (Fig. 11).

iii) They have also presented new accurate multiplicity distributions at several cm energies, which show impressive evidence for KNO scaling (Fig. 12). It should be noted that the shape of the "universal" KNO scaling function is in general different for e^+e^- and for hadron interactions.

iv) The CELLO Collaboration has presented new evidence for scaling violation of the fragmentation function[39]. It agrees with earlier measurements of TASSO[39], MARK II [39], and JADE [38].

3.3 Particle Composition

The particle composition of the hadronic final state has now been measured over the whole momentum range. The CELLO, JADE and TASSO experiments have made contributions. The results for a CM energy of 34 GeV are shown in Table 3.1.

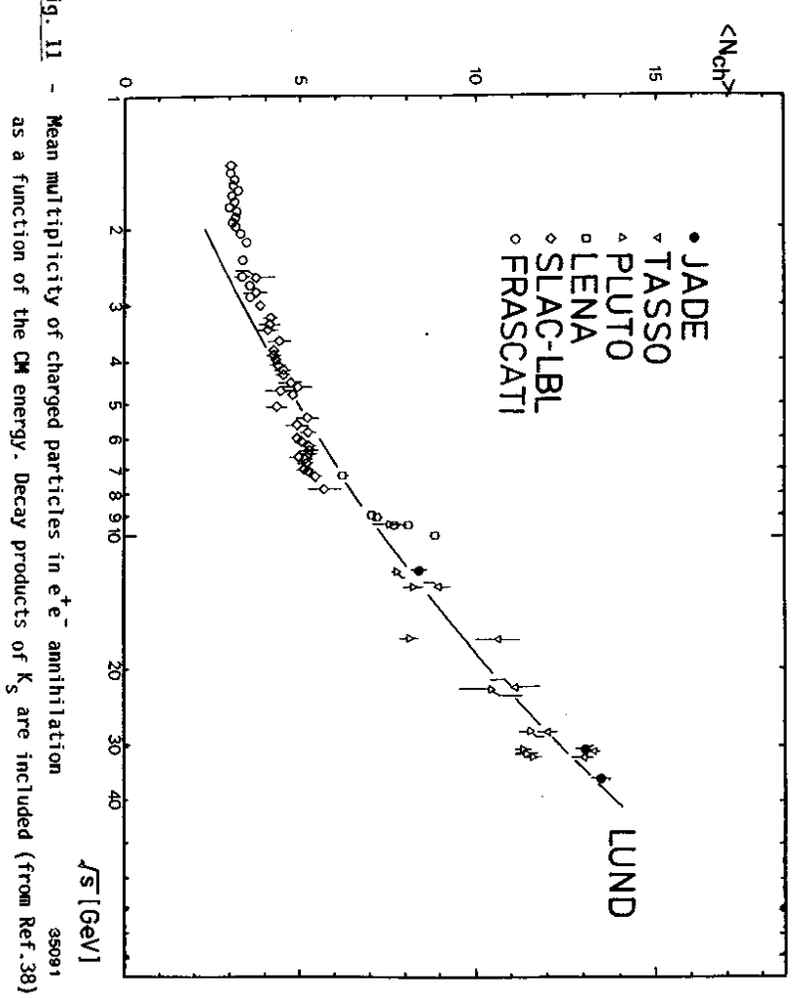

Fig. 11 - Mean multiplicity of charged particles in e^+e^- annihilation as a function of the CM energy. Decay products of K_s are included (from Ref.38).

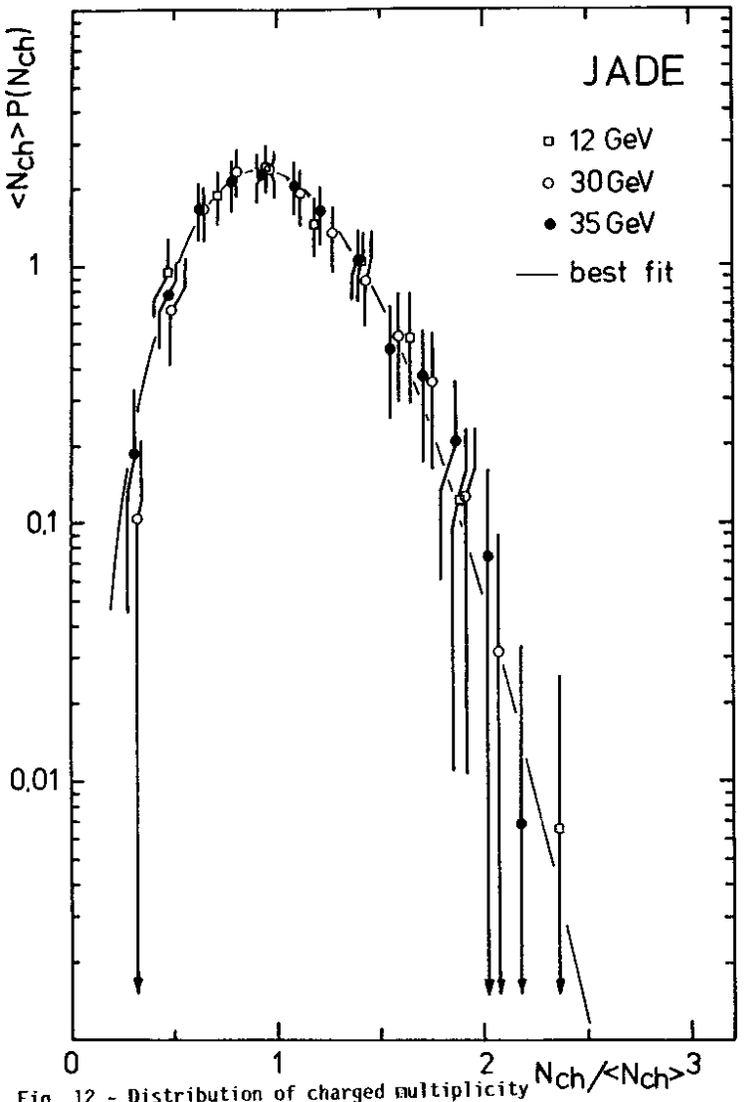

Fig. 12 - Distribution of charged multiplicity at various CM energies (Ref.38). The data follow KNO SCALING: Also shown is the fit to the KNO function used by PLUTO (Phys.Lett.81B(1979)410). 35078

Table 3.1 - Mean Number of Particles produced at 34 GeV cm Energy

Particle i	$\langle n_i \rangle$	reference
$\pi^+ + \pi^-$	10.3 ± 0.4	TASSO[40]
π^0	6.1 ± 2.0	TASSO[41]
	5.2	CELLO[42]
η	$.72 \pm .10 \pm .18$	JADE[43]
ρ^0	$.73 \pm 0.06$	TASSO[44]
	$.82 \pm .12 \pm .10$	JADE[45]
$K^+ + K^-$	2.0 ± 0.2	TASSO[40]
$K^0 + \bar{K}^0$	1.6 ± 0.1	TASSO[46]
	1.45 ± 0.17	JADE[45]
$K^{*+} + K^{*-}$	$.83 \pm .18 \pm .13$ (prelim.)	JADE[45]
$D^{*+} + D^{*-}$	$.31 \pm .07 \pm .11$	TASSO[20]
$p + \bar{p}$	0.8 ± 0.1	TASSO[40]
$\Lambda + \bar{\Lambda}$	0.28 ± 0.04	TASSO[47]
$\Xi^- + \bar{\Xi}^-$	$0.026 \pm 0.008 \pm 0.009$	TASSO[48]

*) from a comparison of $\pi^+\pi^-$ and π^0 data Fig. 13, assumed to be $(\pi^+ + \pi^-)/2$.

In addition to the published results of TASSO there are a number of important new contributions. Fig. 13 shows a new measurement[42] of the π^0 momentum spectrum, made by CELLO with their lead-liquid argon shower counter. It is compared with the TASSO π^+, π^- and the π^0 meson are seen to agree with the average of π^+ and π^-.

Fig. 14 shows evidence for the η mesons, obtained by JADE with their lead glass shower counter. Fig. 14a shows the π^0 signal in the $\gamma\gamma$ invariant mass distribution and a shoulder at the η mass. A lower limit of 200 MeV for the photon energy was applied. If one omits those photons, which are part of a $\gamma\gamma$ mass combination in the π^0 mass band, and whose energy is above 300 MeV, one obtains Fig. 14b, where the η signal is seen more clearly, because the combinatorial background has been reduced. Fig. 14c shows the background subtracted $\gamma\gamma$ mass distribution in the η region with a clear signal. Fig. 15 shows the $K^{*\pm}$ signal of JADE in the $K^0_S\pi^\pm$ mass distribution.

Fig. 16 shows the evidence for the production and decay of the Ξ^- / ($\bar{\Xi}^-$) hyperon, obtained by the TASSO Collaboration. Fig. 16a shows a clear peak at the Ξ^- mass in the combined $\Lambda\pi^-$ and $\bar{\Lambda}\pi^+$ mass distributions. As a check the "wrong" combinations $\Lambda\pi^+$ and $\bar{\Lambda}\pi^-$ are plotted in Fig. 16b, and no signal is seen there.

Consequently, we have now a rather complete overview on the particle composition of the hadronic final state.

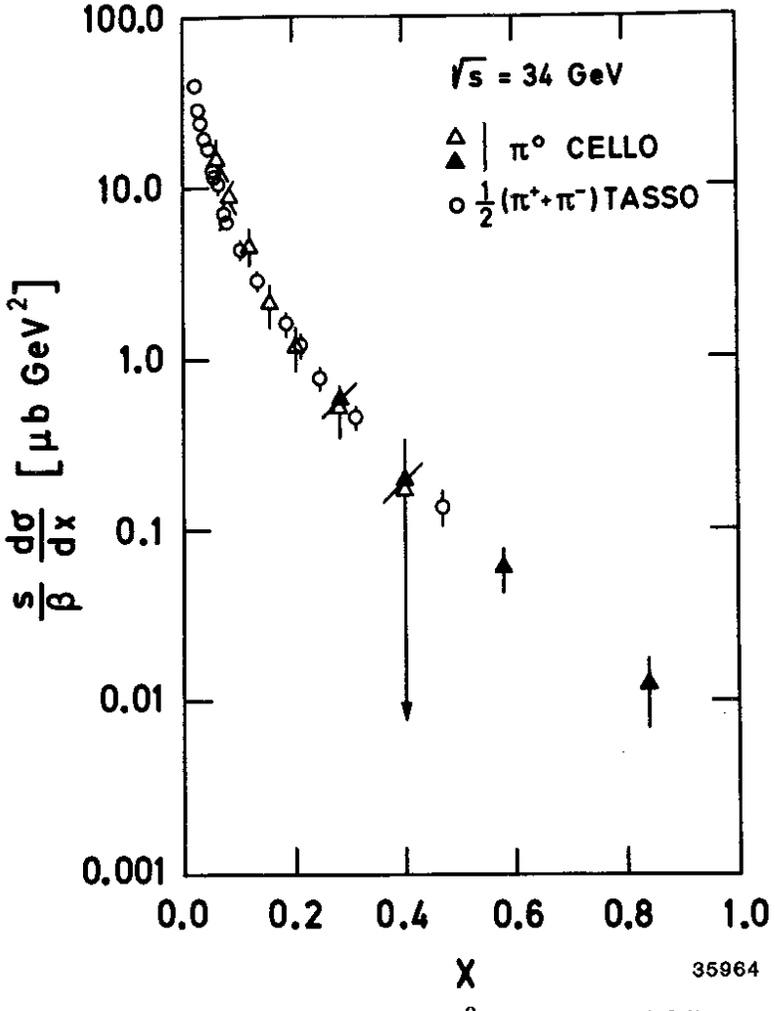

Fig. 13 - Inclusive cross section for π^0 production at 34 GeV CMS energy (Ref. 42) $x = 2E(\pi^0) / E_{CM}$.

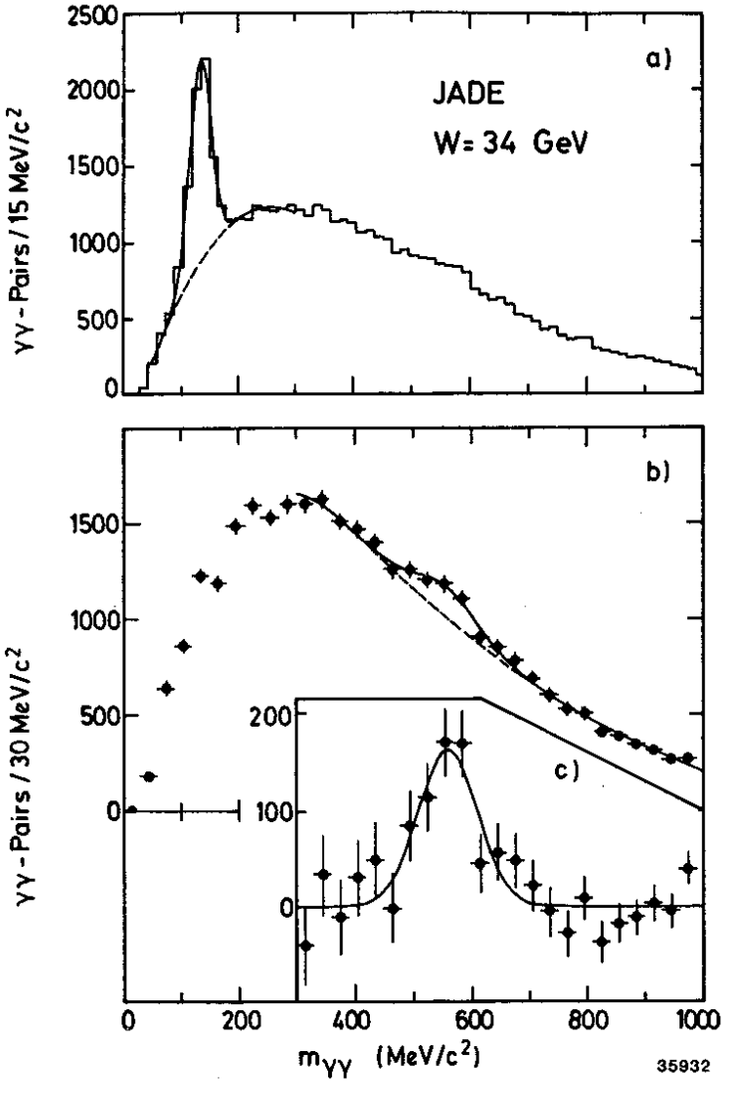

Fig. 14 - Inclusive η production at 34 GeV CMS energy
a) γγ-mass distribution b) with cuts (see text)
c) background subtracted signal (Ref.43).

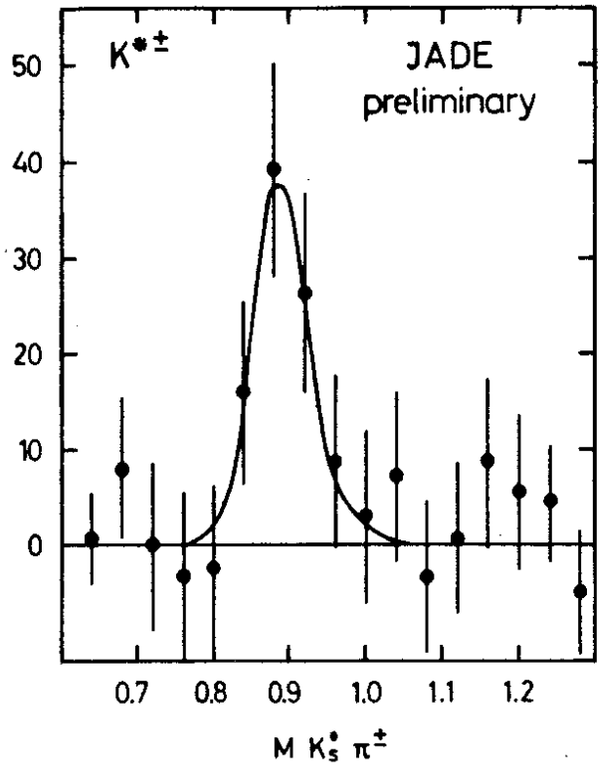

Fig. 15 - K^0_s-$\pi^\pm$ mass distribution, after background subtraction (Ref. 45).

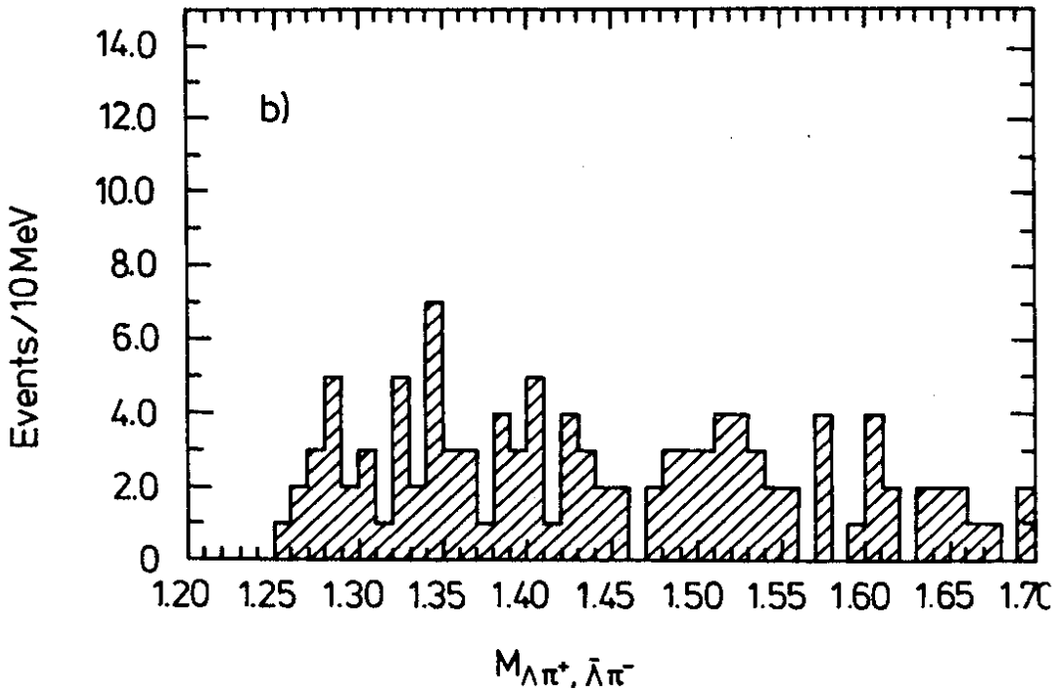

Fig. 16 b - Check with $\bar{\Lambda}\pi^-$, $\Lambda\pi^+$ mass distribution TASSO, Ref. 48.

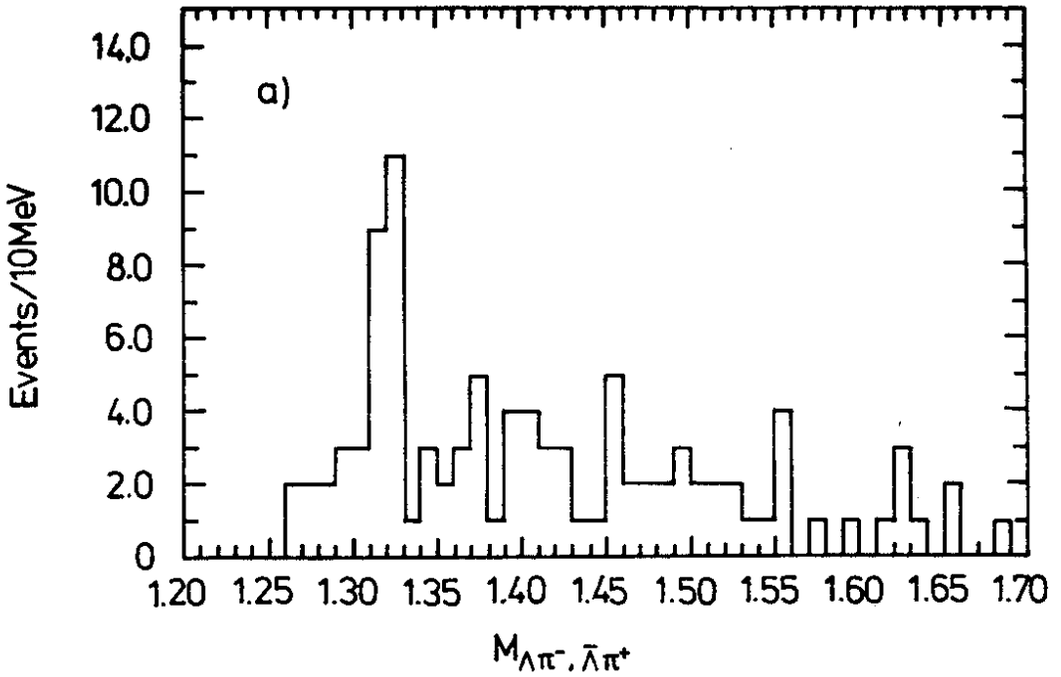

Fig. 16a - Evidence for Ξ^- ($\bar{\Xi}^-$) production in the $\Lambda\pi^-$, $\bar{\Lambda}\pi^+$ mass distribution.

A few simple remarks are the following:

i) The question of how many "particles" are produced on average requires a careful definition. Certainly the total number of hadrons produced on average in a e^+e^- collision is not the sum of the numbers in Table 3.1, because some of those particles may be decay products of other hadrons. For example, the listed number of $\pi^+ + \pi^-$ includes those pions, which come from the decay of K^0_S, Λ, D, D*, ρ^{0+-} etc. Assuming equal numbers of ρ^+, ρ^- and ρ^0 produced, and similar equalities for the other resonances, one finds from Table 3.1 that at least 70% of the pions come from the decay of heavier hadrons. Likewise one finds that about 20% of the protons come from Λ decay.

ii) Consider the number of kaons produced in the first step of the annihilation reaction $e^+e^- \to q\bar{q}$. The $q\bar{q}$ pair will be $c\bar{c}$ in the fraction 4/11 of the cases, it will be $s\bar{s}$ in the fraction 1/11 of the cases, and the same fraction holds for $b\bar{b}$. Neglecting baryon production, and assuming that each c, s or b quark will ultimately give rise to a kaon, one expects on average 2 x (4/11 + 1/11 + 1/11) = 1.09 kaons/event, arising from the first direct $q\bar{q}$ pair. The total number of kaons found however is 3.5. This means, that only about 30% of the kaons come from the original $s\bar{s}$, $c\bar{c}$, $b\bar{b}$ - quark pairs, and about 70% of the kaons are produced in the subsequent hadronization step.

iii) Assuming equal numbers of $p\bar{p}$ and $n\bar{n}$, and noting that every baryon will finally end up as p or n, one sees that on average 0.8 baryon pairs are produced per event.

iV) Observation of the Ξ^- puts new important constraints on fragmentation models because we now know the fraction of strange particles among the hadrons and we know some fractions of baryon species with strangeness 0, -1 and -2, and these numbers have to be accommodated with a small number of input parameters for the models.

3.4 Properties of Jets

i) Properties of gluon jets: The JADE Collaboration[49] has updated earlier work, in which they look at the transverse momentum of particles relative to the jet axis in three-jet events. They find, that particles in the least energetic of the three jets have a larger mean transverse momentum than those in the two other jets, if normalized to the same jet energy (Fig. 17). Since the least energetic jet has a larger probability to be the gluon jet than the other two jets, this indicates that the particles in gluon jets have a larger mean transverse momentum than those in quark jets.

In addition the particle composition may be different in gluon jets. There are indications, that gluon jets may contain more η's (JADE) and more Λ's (TASSO) than quark jets, but they are at present at the statistical level of 2 - 3 standard deviations.

ii) Comparison of string (Lund-) model and independent parton (Feynman-Field-) model of fragmentation: The JADE Collaboration[49] has updated earlier work in which they have looked at the energy flow of three-jet events in the event plane. Fig. 18 shows, that the pattern fits better the string model than the independent parton model. Fig. 19 shows, that the low energy particles in a jet define a different jet axis from the one of the high energy particles. Assuming one has assigned the low energy particles correctly to the jets, this observation would again favor the string model.

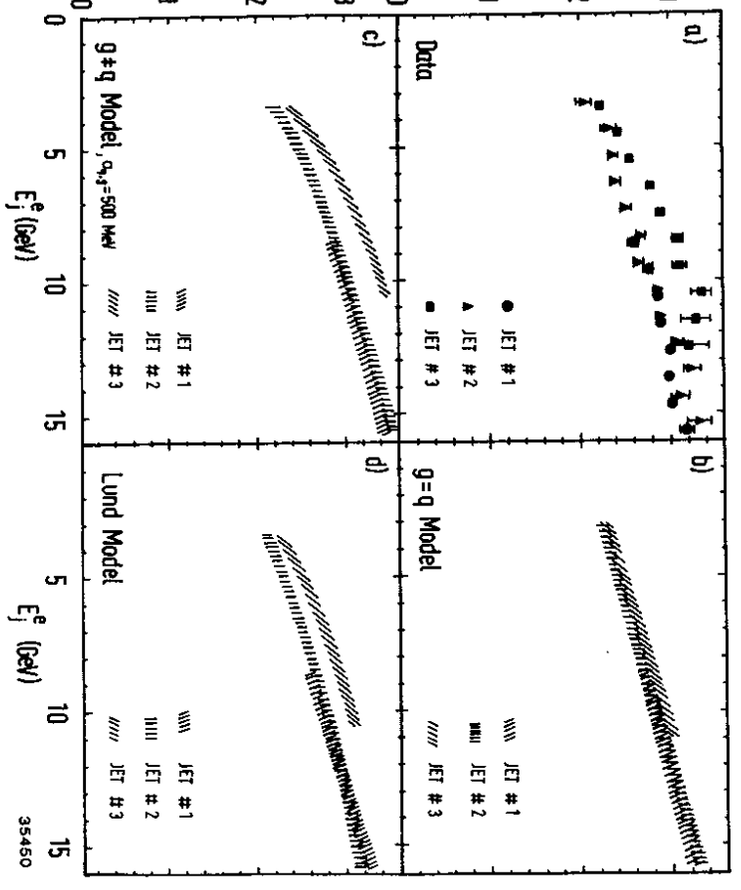

Fig. 17 - Average transverse momentum of charged and neutral particles within a jet relative to the jet axis as a function of jet energy E_j for a) experimental data b,c,d) different models (Ref.49).

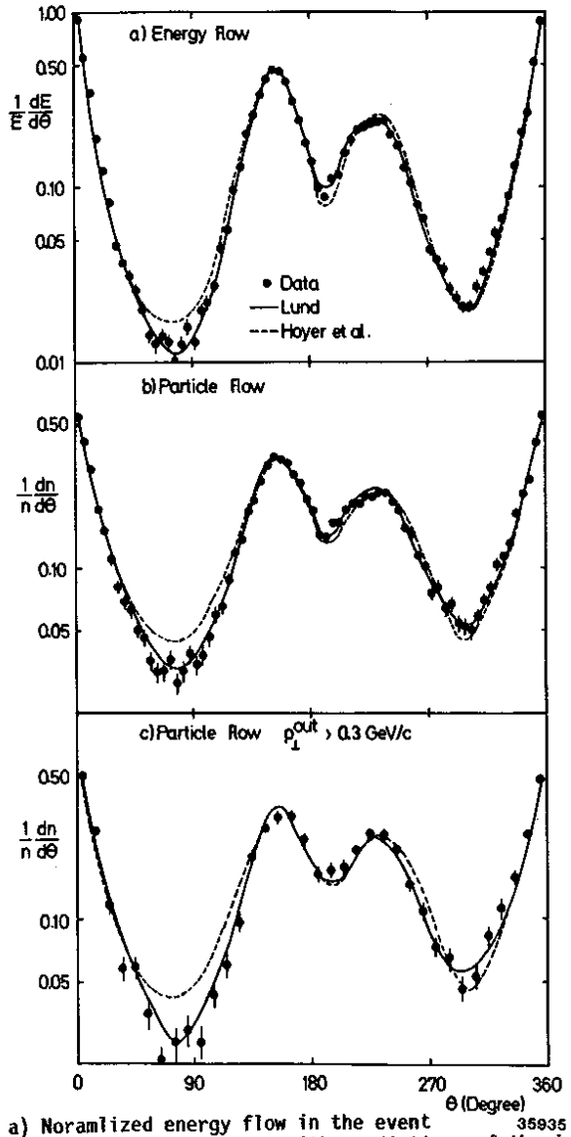

Fig. 18 - a) Noramlized energy flow in the event plane of three jet events together with predictions of the independent parton model (Hoyer et al.) and the string model (Lund) b) Normalized charged and neutral particle flow c) normalized charged and neutral particle flow for particles with $p_{\perp o}$(out) > 0.3 GeV <Ref.49). 35935

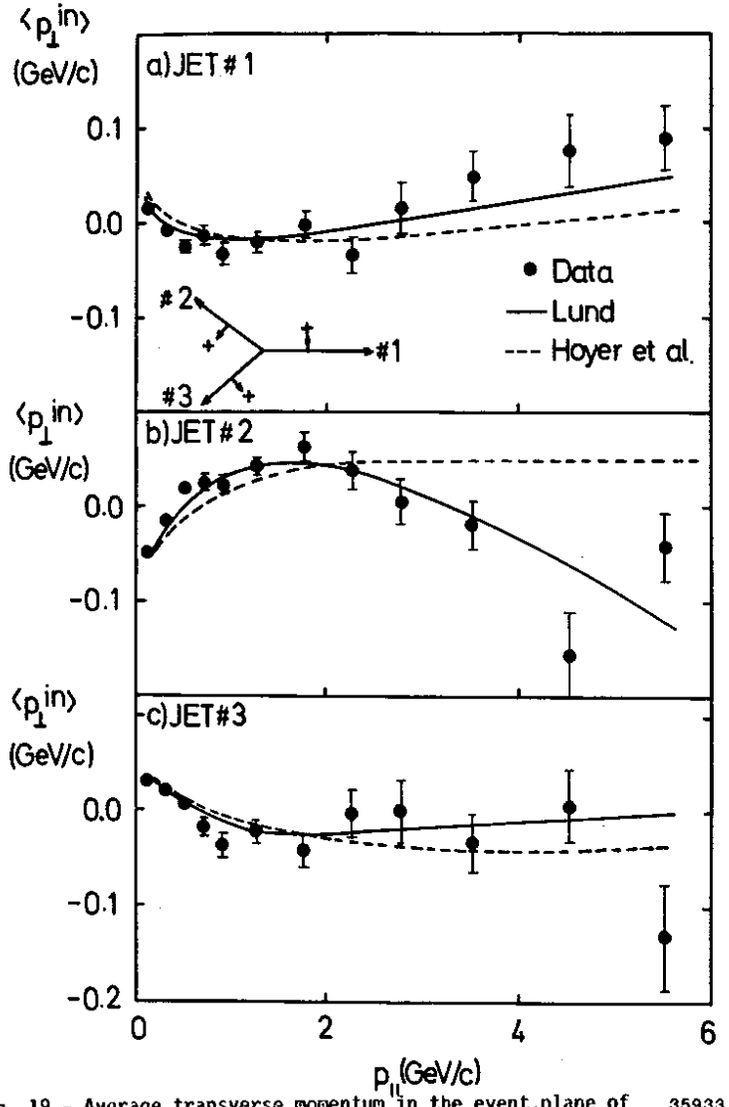

Fig. 19 - Average transverse momentum in the event plane of three jet events with respect to their jet axis $\langle p_\perp^{in} \rangle$ as a function of the momentum component parallel to the jet axis for charged and neutral particles of jets 1, 2, and 3. The sign convention is sketched as well (Ref.49). 35933

3.5 Baryon Number Compensation

The TASSO Collaboration has investigated events with two identified protons and/or antiprotons[50]. The protons (antiprotons) were required to have relatively large momenta ($p > 1$ GeV/c), they were identified by time-of-flight and by Cerenkov counters. Table 3.2 shows the resulting number of events after a background subtraction of misidentified protons (antiprotons). The two particles in the combinations pp or $p\bar{p}$ or $\bar{p}\bar{p}$ may originate in the same jet or in opposite jets. Events of the type pp or $\bar{p}\bar{p}$ must have two or more baryon-antibaryon pairs produced, whereas events of the type $p\bar{p}$ have predominantly a single baryon-antibaryon pair. It is evident from the table, that for the $p\bar{p}$ combination the two particles have a strong tendency to originate from the same jet, pointing towards a local compensation of baryon number in the hadronization process.

Table 3.2 - Proton- (Anti-) Proton Correlations

Pairing	Number of events with the two particles in the	
	same jet	opposite jet
pp or $\bar{p}\bar{p}$	-0.2 ± 2.1	2.7 ± 3.1
$p\bar{p}$	15.0 ± 4.6	3.0 ± 3.0

3.6 Fragmentation Function of Heavy Quarks

There are two methods to obtain information on the momentum distribution of the c- and b-quarks.

i) The first method identifies these heavy quarks by the semi-leptonic decays of the respective hadrons (assumed to be mostly D- or B-mesons). The inclusive momentum spectra of electrons and/or muons are fitted to the theoretical decay spectrum of D- or B-mesons, folded with different assumed distributions for the D- or B-momenta, see section 2.2 for experimental details.

This method is somewhat indirect and requires delicate background subtractions. Moreover, it measures by definition the momentum distribution of the lightest meson species of a given flavor, which may be the decay product of heavier resonant states. As an example, look at Table 3.1, which indicates, that a large fraction of c-quark production may be in the form of the D*-resonance.

ii) The second method identifies the D- or B-mesons directly. This is good in principle, but severely limited by statistics and/or failure to resolve the D- or B-mass peaks. So far it has worked only for the case of the D* .

The results are given in Table 3.3 in terms of the average value of z, where

$$z = p / E_b$$

and p = momentum of the D- or B-meson, E_b = beam energy.

Table 3.3 - Average values of z for mesons containing a c- or b-quark

Experiment	$\langle z_c \rangle$	$\langle z_b \rangle$	$\langle z_{D^*} \rangle$	Method
MARK-J[23]	$.46 \pm .02 \pm .05$	$.75 \pm .03 \pm .06$		(i)
TASSO[50]			$.57 \pm .04$	(ii)

4. TWO PHOTON PHYSICS

4.1 Two Photon Decay Widths of Mesons

The Feynman diagram Fig. 20 shows the principle of the method.

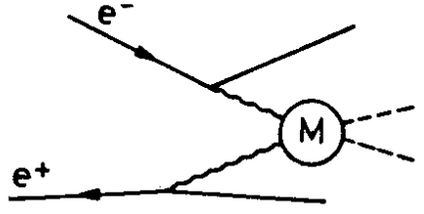

Fig. 20

One observes the cross section for the reaction

$$e^+e^- \to e^+e^- \; \gamma\gamma, \quad \gamma\gamma \to M$$

where γ is an almost real photon, M is a meson, which is identified by its decay. This cross section can be connected to the width $\Gamma_{\gamma\gamma}$ of the decay of the meson M into two photons. The approximate relation for the total production cross section of the meson M is[52]:

$$\sigma(e^+e^- \to e^+e^-M) \simeq 2\left(\frac{\alpha}{\pi} \ln \frac{E}{m_e}\right)^2 \int_0^{4E^2} \frac{ds}{s} f\left(\frac{\sqrt{s}}{2E}\right) \sigma(\gamma\gamma \to M(s))$$

with $\sigma(\gamma\gamma \to M) = 8\pi^2 (2J+1) \cdot \frac{\Gamma(M \to \gamma\gamma)}{M_r} \delta(s - M_r^2)$ we have

$$\sigma(e^+e^- \to e^+e^-M) \simeq 2\left(\frac{\alpha}{\pi} \ln \frac{E}{m_e}\right)^2 \cdot 8\pi^2 (2J+1) \frac{\Gamma_{\gamma\gamma}}{M_r^3} f\left(\frac{M_r}{2E}\right) \quad (7)$$

where E = beam energy, M_r and J are the mass and the spin of the meson, $f(x) = (2+x^2)^2 \ln\left(\frac{1}{x}\right) - (1-x^2)(3+x^2)$

Results are shown in Table 4.1.

Table 4.1 - Two-Photon Decay Widths[53)]

Experiment	$\Gamma(f \to \gamma\gamma)$ keV	Remarks
MARK II	$3.6 \pm 0.3 \pm 0.5$	$f \to \pi^+\pi^-$
CELLO	$2.5 \pm 0.1 \pm 0.5$	$f \to \pi^+\pi^-$
XALL BALL	$2.9 \begin{smallmatrix}+0.6\\-0.4\end{smallmatrix} \pm 0.6$	$f \to \pi^0\pi^0$
JADE	$2.3 \pm 0.2 \pm 0.5$ (preliminary)	$f \to \pi^0\pi^0$
TASSO	$3.2 \pm 0.2 \pm 0.6$	$f \to \pi^+\pi^-$
PLUTO	$2.3 \pm 0.5 \pm 0.35$	$f \to \pi^+\pi^-$
	$\Gamma(A_2 \to \gamma\gamma)$ keV	
CELLO	$0.81 \pm 0.19 \begin{smallmatrix}+0.42\\-0.11\end{smallmatrix}$	
JADE	$0.84 \pm .07 \pm .15$ (preliminary)	
Xall ball	$0.77 \pm 0.18 \pm 0.27$	
	$\Gamma(f' \to \gamma\gamma)$ keV	
TASSO	$0.11 \pm 0.02 \pm 0.04$	
	$\Gamma(\eta' \to \gamma\gamma)$ keV	
PLUTO	$3.7 \pm 0.2 \pm 0.6$	preliminary
JADE	$5.0 \pm 0.5 \pm 0.9$	
CELLO	$6.2 \pm 1.1 \pm 0.8$	
TASSO	$4.1 \pm 0.4 \pm 1.5$	preliminary
MARK II	$5.8 \pm 1.1 \pm 1.2$	

Remarks:

(i) There has been a difficulty on the fits of the f-mass distribution, the fitted mass value coming out too low. From recent CELLO work this now seems better understood.

(ii) Flavor SU_3 gives a relation between the widths of the 2^{++}-mesons f, A_2 and f'. The data are in agreement with a mixing angle of about 30°, close to ideal mixing.

(iii) The η' width $\Gamma(\eta' \to \gamma\gamma)$ agrees with the value ~ 5 keV expected from the standard quark model.

4.2 Production of Hadron Pairs

The reaction of interest is

$$\gamma + \gamma \to h\bar{h}$$

where the two photons are almost real and $h\bar{h}$ is a hadron-anti-hadron pair. For large values of the $h\bar{h}$ invariant mass, this process can in principle be calculated with perturbative QCD (see Fig. 21). There are now first experimental and theoretical results, and they are interesting, but not too much should be expected in the way of accuracy at the present time.

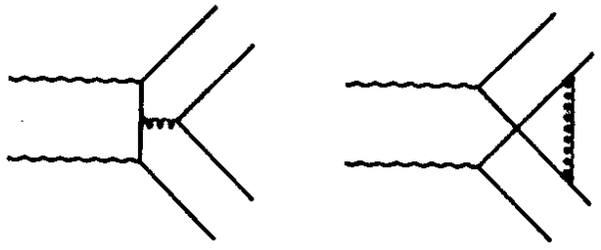

Fig. 21

Some Feynman Diagrams for computing the process $\gamma\gamma \to h\bar{h}$, h being a meson.

The TASSO and CELLO Collaborations[54] have measured the reaction $\gamma\gamma \to \rho^0\rho^0$. The results are shown in Fig. 22. Considering the difficulty of the measurement, there is reasonable agreement. The JADE Collaboration[54] has tried to measure $\gamma\gamma \to \rho^+\rho^-$. This cross section is small, and they have only obtained upper limits, which are also shown in Fig. 22. The JADE measurement puts severe constraints on models, which have tried to explain the relatively large cross section for $\gamma\gamma \to \rho^0\rho^0$ at low energies by resonance formation.

The TASSO Collaboration[55] has measured the reaction $\gamma\gamma \to p\bar{p}$. Fig. 23 shows their result. The cross section is smaller by an order of magnitude than the value obtained from a naive calculation using a pointlike proton, and it seems to agree within a factor of 2 - 3 with a QCD calculation by Damgaard[56].

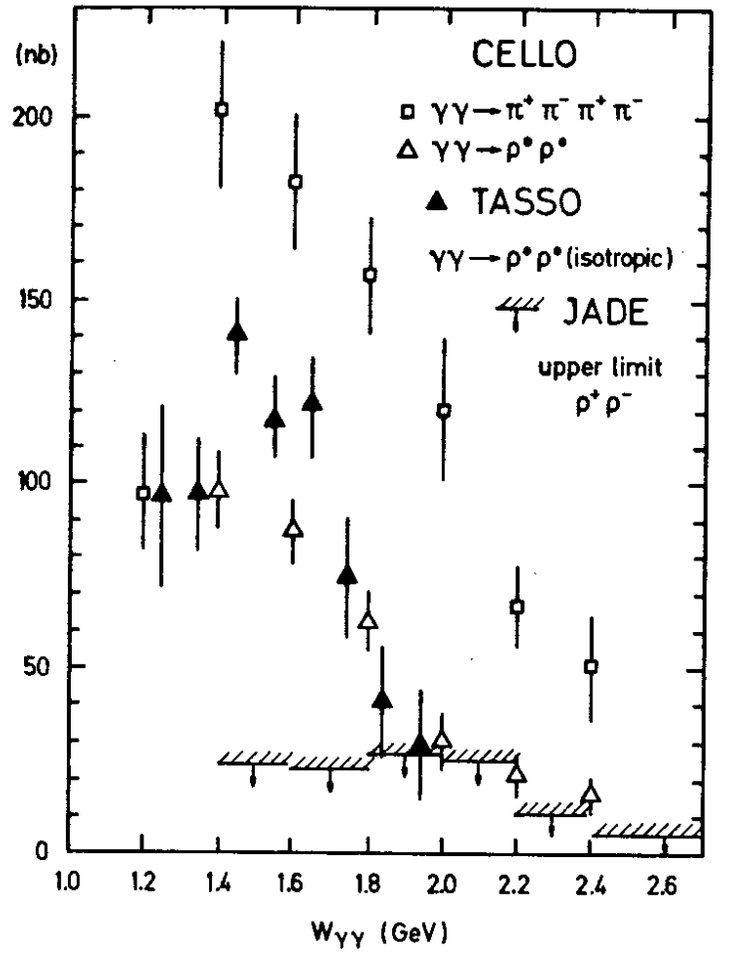

Fig. 22 - Cross section for the reaction $\gamma\gamma \to \rho^0\rho^0$ and $\gamma\gamma \to \rho^+\rho^-$ as function of the $\gamma\gamma$ CM energy $W_{\gamma\gamma}$.

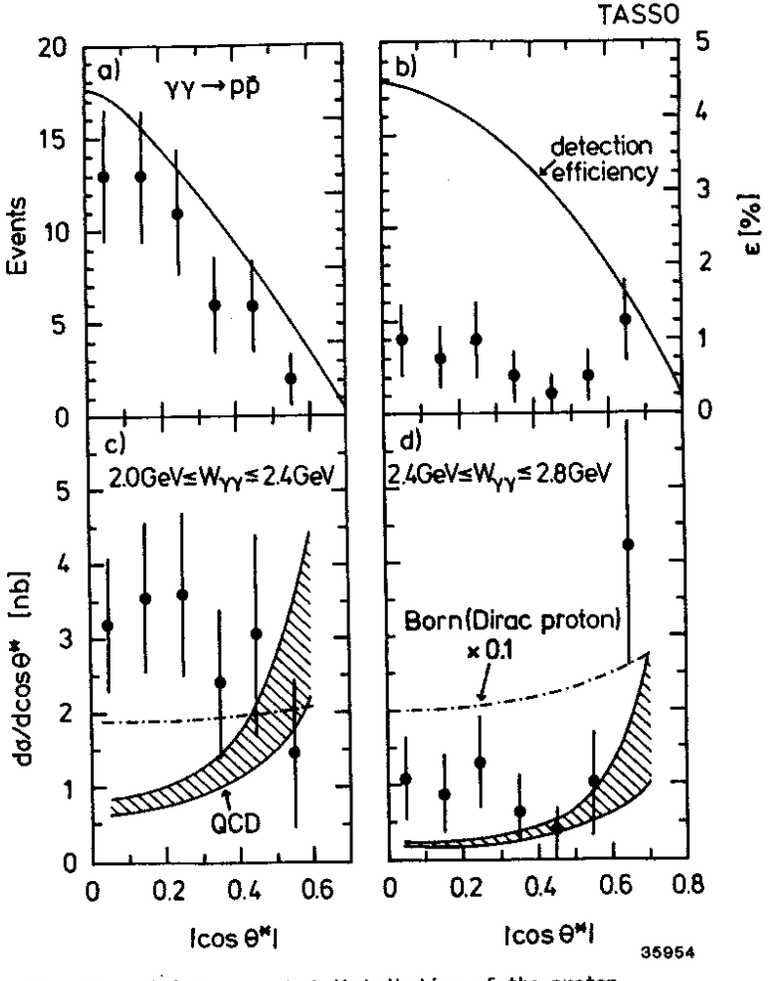

Fig. 23 - a)b) Uncorrected distribution of the proton scattering angle in the γγ CM system, and detection efficiency c)d) differential crosss section of γγ → pp̄; the data are compared with the Born approximation for Dirac protons and with Ref. 56.

The PLUTO Collaboration has measured the reaction

$$\gamma\gamma \rightarrow h^+h^-$$

with $h^\pm$ being mostly $\pi^\pm$.

Their result for a h^+h^- invariant mass $W > 2$ GeV/c^2 is[57]:

$$\frac{(e^+e^- \rightarrow e^+e^- h^+h^-)}{(e^+e^- \rightarrow e^+e^- \mu^+\mu^-)} = 0.061 \pm 0.019 \pm 0.015$$

to be compared with the value 0.020 ± 0.01 expected from a QCD calculation [58],

4.3 Photon Structure Function

Consider the process $e^+e^- \rightarrow e^+e^-\ \gamma\gamma \rightarrow e^+e^-$ + hadrons described in its simplest version by the Feynman diagram Fig. 24a.

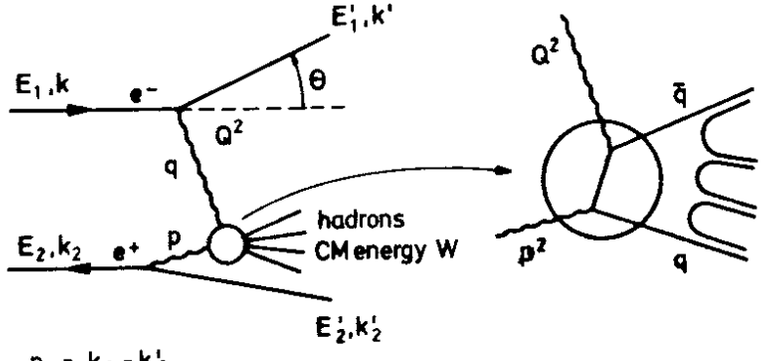

$\underline{p} = \underline{k}_2 - \underline{k}'_2$

$\underline{q} = \underline{k} - \underline{k}'$

$E_\gamma = E_2 - E'_2$

a) b)

Fig. 24

If one of the photons has a large absolute value Q^2 of the four momentum transfer squared, and if the cm energy W of the hadrons is large, then one expects that the quark parton model as shown in the diagram in Fig. 24b will give the main contribution to the cross section. The cross section then becomes calculable by the quark parton model or by QCD if gluon effects are included.

If one of the two photons has a small value q^2 of the four momentum transfer squared ($|q^2| < M^2$), and the other one has a large value Q^2, the process can - if one likes - be viewed as the deep inelastic scattering of an electron with momentum transfer Q^2 off an almost real "target" photon, and the cross section formulae can be cast into a form similar to those for deep inelastic scattering. With the symbols as explained in Fig. 24a, one has for the inelastic scattering of an electron off an (almost) real photon of energy E_γ [59].

$$\frac{d^2\,\sigma(e\gamma \to e\ \text{hadrons})}{dxdy} = \frac{16\pi\,\alpha^2}{Q^4} \cdot E_1\,E_\gamma \cdot [(1-y)F_2(x,Q^2)+xy^2F_1(x,Q^2)] \qquad (8)$$

with

$Q^2 = -(\underline{k} - \underline{k}')^2 \cong E_1E_1' \sin^2\theta/2$

$x = Q^2/(2\underline{p}\cdot \underline{q}) \approx Q^2/(Q^2 + W^2)$

$W^2 = (\underline{p} + \underline{q})^2$

$y = (\underline{p} \cdot \underline{q}) / (\underline{k} \cdot \underline{p}) = 1-(E_1' / E_1) \cdot \cos^2\theta/2$

E_1, E_1', E_2, E_2' are electron and positron energies before and after the collision, and $\underline{k}$, $\underline{k}'$, $\underline{k}_2$, $\underline{k}_2'$ are the corresponding four vectors.

Under most experimental conditions, xy^2 is small, so that one can neglect the term with $F_1(x,Q^2)$. The structure function $F_2(x,Q^2)$ can be computed in the quark parton model according to Fig. 24b and one gets [58]

$$F_2^{QPM}(x,Q^2) \cong \frac{3\alpha}{\pi} \cdot \Sigma Q_f^4 \cdot x \cdot [(x^2 + (1-x)^2) \cdot \ln \frac{W^2}{m_q^2} + 8x(1-x)-1] \qquad (9)$$

(a factor 3 for color is included.

Eq.(9) contains the (unknown) masses of the quarks. As one includes the effect of gluons, one gets the following expression for the photon structure function in QCD:

$$F_2^{QCD}(x, Q^2) \cong \frac{3\alpha}{\pi}\,\Sigma Q_f^4 \ln \frac{Q^2}{\Lambda^2} \cdot h(x) \qquad (10)$$

where the sum is over the charges Q_f of the quarks considered, there is a factor 3 in the formula for color, h(x) in a calculable function [60] and Λ is the QCD constant. One has therefore - in principle - a process which allows a check of QCD and a determination of Λ.

In practice, there are the following difficulties:

i) It is experimentally difficult to measure W, the total hadronic energy, because this requires very good solid angle coverage and calorimetry. The deficiencies of the detector have to be corrected by more or less critical Monte Carlo calculations. Since W enters into the expression for x, there is a difficulty in knowing x.

ii) There are still difficulties in computing the QCD part, especially at finite values of Q^2.

iii) There is an ambiguity in how to include the heavy quarks. It has been customary to describe the u, d, s - quarks by QCD (Eq. 10), and the c, b - quarks by Eq.9.

There is a hadronic-vector-meson-dominance-like part of the photon, which is not described by the QCD mechanism, and which can be approximated by an addition to the QCD structure function, namely[61]:

$$F_2^{VDM}(x,Q^2) \cong \alpha \cdot 0.2 \cdot (1-x) \qquad (11)$$

The data have to be fit to a sum of Eq.11 and Eq.9 and/or Eq.10.

In spite of these difficulties measurements of deep inelastic electron-photon scattering may finally offer a very good check of QCD. First encouraging measurements have been made by the CELLO, JADE and PLUTO Collaborations. As a first check on the experimental procedure one measures[62] the cross section for $e^+e^- \to e^+e^-\,\mu^+\mu^-$, $e^+e^-e^+e^-$ which is very similar on the parton level and which can be calculated in QED (see Fig. 25). Measurements of the photon structure function are shown in Fig. 26 and Fig. 27. They are in agreement with a value of Λ between 100 MeV and 300 MeV, as are measurements by CELLO[66].

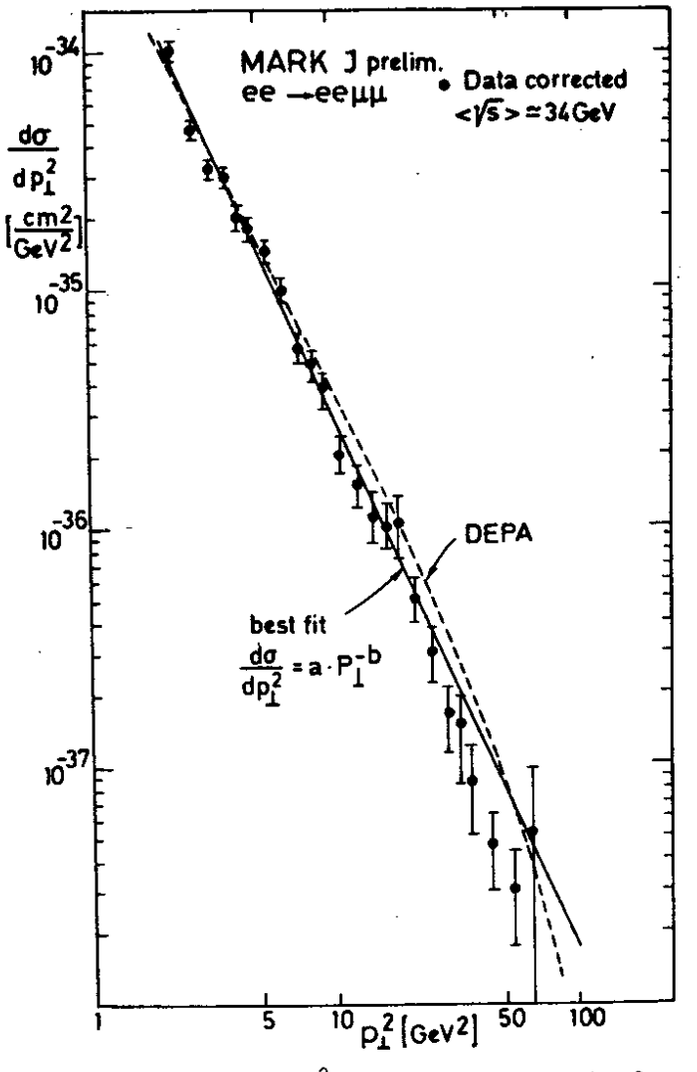

Fig. 25 - Cross section $d\sigma/dp_\perp^2$ for two photon muon pairs from MARK-J. The data are compared to a DEPA[63] calculation and fitted to a power law (from Ref. 62).

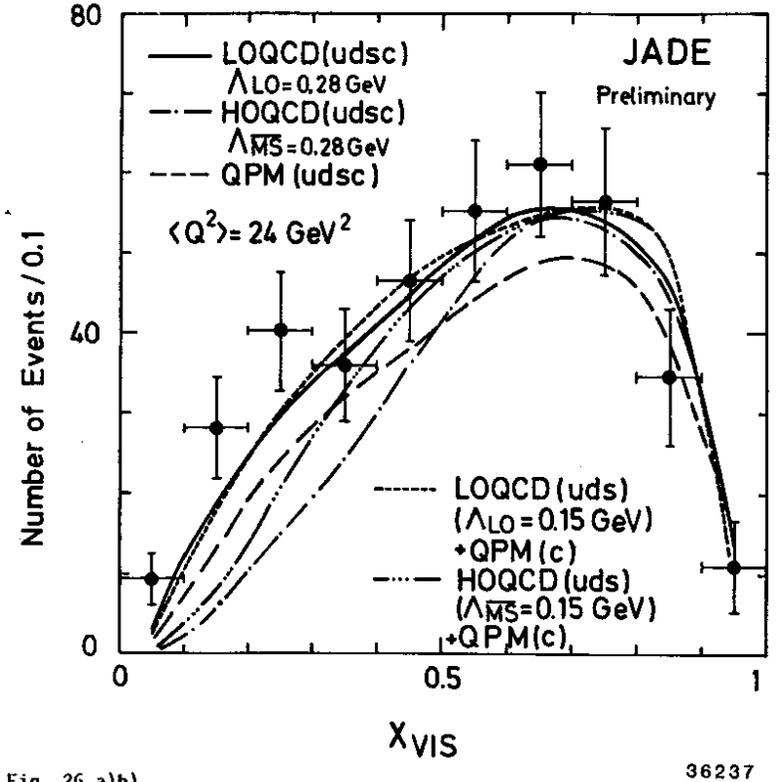

Fig. 26 a)b)

Photon structure function as a function of X_{VIS}, the value of x computed from the visible hadron energy W_{VIS}, at two different values of average Q^2 from JADE[65]. Comparison with various theoretical models LOQCD (leading order QCD Ref. 60), HOQCD (higher order QCD Ref.64), QPM = Quark parton model Eq.9.

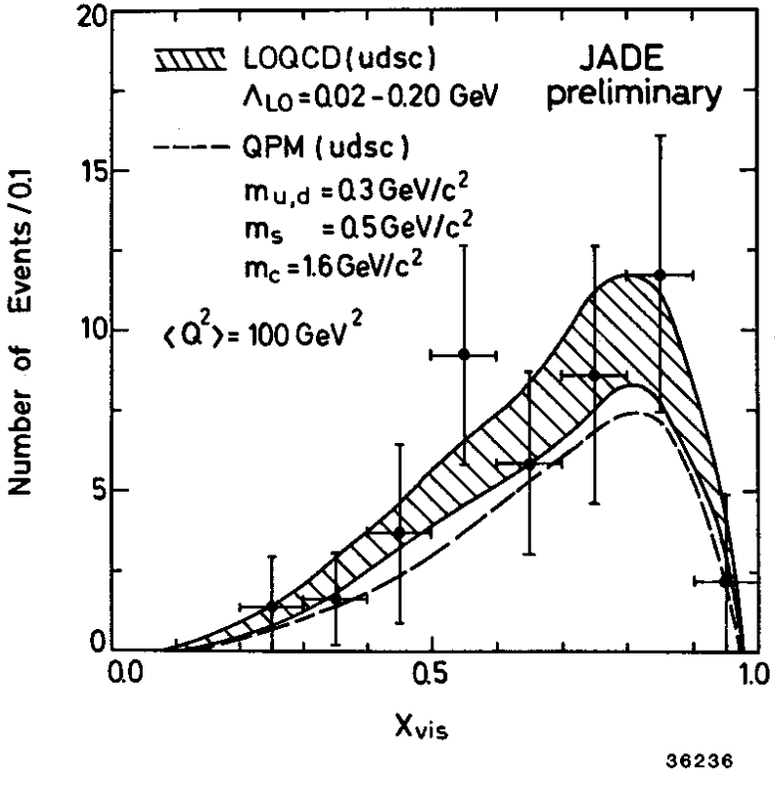

Fig. 26 b - Captions see Fig. 26a

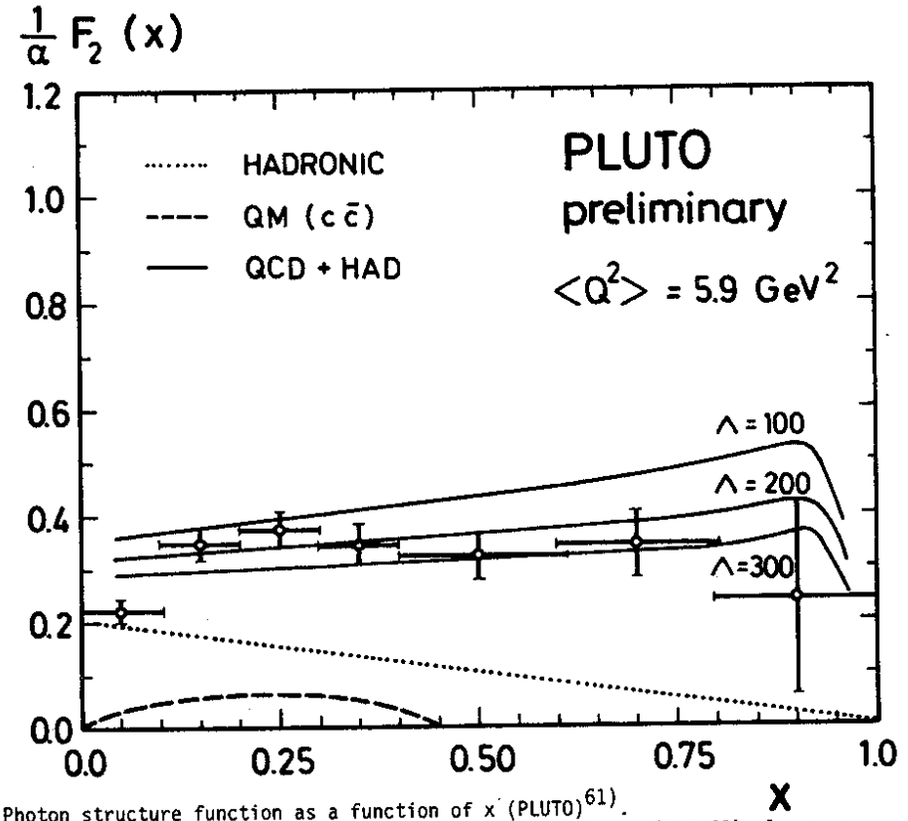

Fig. 27 - Photon structure function as a function of x (PLUTO)[61]. The data are compared with leading order QCD calculations (Ref.60) plus hadronic part (eq.11).

Acknowledgements

I like to thank Dr. R.Felst, Dr. G.Wolf, Dr. U.Timm, Prof. G.Flügge, Prof. A.Böhm and Dr. W.Wagner for their help in preparing this talk and for discussions and criticism. I also thank Dr. B.Naroska for useful comments. - Finally I thank the organizers of the SLAC Summer Study for a most stimulating and inspiring meeting.

REFERENCES

1) A.Böhm, DESY Report 82-027

2) J.Bürger, 1981 Int.Symp. on Lepton and Photon Int. at High Energies, Bonn, Germany,

3) S.Yamada, DESY report 83-056 and Review talk at the 1983 Cornell Conference on Lepton and Photon Int. at High Energies,

4) MARK-J, B.Adeva et al., Contribution to the 1983 Cornell Conference,

5) TASSO Collaboration, Contribution to the 1983 Cornell Conference,

6) K.Kinoshita, P.B.Price and D.Fryberger, Phys.Rev.Lett. 48 (1982) 77

7) P.Musset, M.Price and E.Lohrmann, Phys.Lett. 128B (1983) 333

8) JADE Collaboration, contribution to the 1983 Cornell Conference, see also Ref. 3),

9) Yu.A.Gel'fand and E.P.Likhtman, JETP Letters 13 (1971) 323
J.Wess and B.Zumino, Nucl.Phys. B70 (1974) 39
P.Fayet and S.Ferrara, Phys.Rep. 3C (1977) 249,

10) CELLO Collaboration, H.-J.Behrend et al., Phys.Lett. 123B (1983) 127,

11) JADE Collaboration, W.Bartel et al., Phys.Lett. 114B (1982) 211
CELLO Collaboration, H.-J.Behrend et al., DESY 82-021
MARK-J Collaboration, A.Adeva et al., LNS Tech.Rep. 125 <1982)
MARK-II Collaboration, C.A.Blocker et al., SLAC-PUB-2923 (1982)
MAC Collaboration, Proc. Int. Conference on High Energy Physics, Paris 1982

12) TASSO Collaboration, M.Althoff et al., Phys.Lett. 122B (1983) 95,

13) J.Ellis and M.K.Gaillard, CERN Rep. 76-18 (1976)
J.Jersak, E.Laermann and P.M.Zerwas, Phys.Lett. 98B (1981) 363
Th.Appelquist and H.P.Politzer, Phys.Rev. D12 (1975) 1404

14) JADE Collaboration, Contribution to 1983 Cornell Conference,
MARK-J. Collaboration, Contribution to 1983 Cornell Conference,
PLUTO-Collaboration, Ch.Berger et al., DESY 83-084,
TASSO Collaboration, M.Althoff et al., DESY 83-089,

15) F.A.Berends, R.Kleiss and S.Jadach, Nucl.Phys. B 202 (1982) 63

16) M.Böhm and W.Hollik, DESY 83-060,

17) Review by A.Böhm, DESY 82-084,

18) W.Krenz, Aachen Preprint PITHA 82-26,

19) MARK-J. Collaboration, D.P.Barber et al., Aachen preprint PITHA 80-8, J.J.Sakurai, Proc. 17 Rencontre de Moriond 1982,

20) J.M.Yelton et al., Phys.Rev.Lett. 49 (1982) 430,
CLEO Collaboration, C.Bebek et al., Phys.Rev.Lett. 49 (1982) 610,
TASSO Collaboration, M.Althoff et al., Phys.Lett. 126B (1983) 493,

21) Contributuions to the 1983 Cornell Conference, see Review talk by B.Naroska,

22) CELLO Collaboration, H.-J.Behrend et al., contribution to the 1983 Cornell Conference,

23) MARK-J. Collaboration, B.Adeva et al., Phys.Rev.Lett. 51 (1983) 443,
CELLO Collaboration, H.-J.Behrend et al., Z.Phys. C 19 (1983) 291,
TASSO Collaboration, contribution to the 1983 Cornell Conference,

24) JADE Collaboration, W.Bartel et al., DESY 83-049,
MARK-J Collaboration, B.Adeva et al., Phys.Rev.Lett.50
(1983) 799,
25) H.Georgi and S.Glashow, Nucl.Phys. B 167 (1980) 173,
V.Barger, W.Y.Keung and R.J.N.Phillips, Phys.Rev. D 24
(1981) 1328
G.L.Kane and M.E.Peskin, Nucl.Phys. B 195 (1982) 29,
26) JADE Collaboration, W.Bartel et al., Phys.Lett. 129B (1983) 145
TASSO Collaboration, R.Brandelik et al., Phys.Lett. 113B
(1982) 499,
MARK-J. Collaboration, Review talk by A.Böhm, DESY 82-084,
MAC Collaboration, Contribution to the 1983 Cornell Conf.
27) G.Kramer, DESY 83-068 and DESY 82-029,
T.Gottschalk, Phys.Lett. 109B (1982) 331,
28) G.Wolf, Talk at the Theory Workshop "Hadron and Jet Structure"
DESY, 27th September 1983,
29) CELLO Collaboration, H.-J.Behrend et al., Contribution to
the 1983 EPS Conference in Brighton,
30) CELLO Collaboration, H.-J.Behrend et al., Nucl.Phys. B218
(1983) 269,
31) JADE Collaboration, W.BArtel et al., Phys.Lett. 119B (1982) 239,
32) MARK-J Collaboration, B.Adeva et al., Phys.Rev.Lett. 50
(1983) 2051,
33) TASSO Collaboration, contribution to the 1983 Cornell Conference,
34) R.K.Ellis, D.A.Ross and A.E.Terrano, Phys.Rev.Lett.45
(1980) 1226 and Nucl.Phys. B 178 (1981) 421,

34) continued - J.Vermaseren et al., Nucl.Phys. B 187 (1981) 301,
35) K.Fabricius, G.Kramer, G.Schierholz and I.Schmitt,
Z.Phys. C11 (1982) 315 - see also Ref. 27),
36) PLUTO Collaboration, Ch.Berger et al., Z.Phys. C12 (1982) 1297,
37) PLUTO Collaboration, Ch.Berger et al., DESY 83-040,
K.Konishi, A.Ukawa and G.Veneziano, Nucl.Phys. B157 (1979) 45,
38) JADE Collaboration, W.Bartel et al., DESY 83-042,
39) CELLO Collaboration, H.-J.Behrend et al., contribution to
the 1983 Cornell Conference,
TASSO Collaboration, R.Brandelik et al., Phys.Lett. 114B
(1982) 65,
MARK-II Collaboration, J.F.Patrick et al., Phys.Rev.Lett. 49
(1982) 1232,
40) TASSO Collaboration, M.Althoff et al., Z.Phys. C 17 (1983) 5,
41) TASSO Collaboration, R.Brandelik et al., Phys.Lett. 108B
(1982) 71,
42) CELLO Collaboration, H.-J.Behrend et al., DESY 83-066,
43) JADE Collaboration, W.BArtel et al., DESY 83-063,
44) TASSO Collaboration, R.Brandelik et al., Phys.Lett. 117 B
(1982) 135,
45) JADE Collaboration, W.Bartel et al., Contribution to the
1983 EPS Conference in Brighton,
46) TASSO Collaboration, R.Brandelik et al., Phys.Lett. 94B
(1980) 91,
47) TASSO Collaboration, R.Brandelik et al., Phys.Lett. 105B
(1981) 75,

48) TASSO Collaboration, M.Althoff et al., DESY 83-071,

49) JADE Collaboration, W.Bartel et al., Phys.Lett. 123B (1983) 460;
DESY 83-080,

50) TASSO Collaboration, M.Althoff et al., Contribution to the
1983 EPS Conference in Brighton,

51) MARK-J Collaboration, B.Adeva et al., DESY 83-029 (see Ref.23),

52) H.Terazawa, Rev.Mod.Phys. 45 (1973) 615,

53) f: MARK-II Collaboration, A.Roussarie et al., Phys.Lett.
105 B (1981) 304,
CELLO Collaboration, H.-J.Behrend et al., Contribution to
the 1983 EPS Conference in Brighton,
XALL BALL Collaboration, C.Edwards et al., Phys.Lett. 110B
(1982) 82,
JADE Collaboration, W.Bartel et al., Contribution to the
1983 EPS Conference in Brighton,
TASSO Collaboration, R.Brandelik et al., Z.Phys. C 10 (1981) 117,
PLUTO Collaboration, Ch.Berger et al., Phys.Lett. 94B (1980) 254,
A_2: CELLO Collaboration. H.-J.Behrend et al., Phys.Lett. 114B
(1982) 378, and Erratum Phys.Lett. 125B (1983) 518
JADE: see f
XALL BALL: see f
f': TASSO Collaboration, M.Althoff et al., Phys.Lett. 121B
(1983) 216,
η': PLUTO Collaboration, contribution to the 1983 EPS Con-
ference in Brighton,
JADE Collaboration, W.Bartel et al., Phys.Lett. 113B(1982)190,

53) η' continued:
CELLO: see A_2
TASSO: Contribution to the 1983 EPS Conference in Brighton
MARK-II Collaboration, G.Abrams et al., Phys.Rev.Lett. 43
(1979) 477,
P.Jenni et al., Phys.Rev. D 27 (1983) 1031,

54) TASSO Collaboration, M.Althoff et al., Z.Phys. C16 (1982) 13
CELLO Collaboration, H.-J.Behrend et al., DESY 83-081,
JADE Collaboration, W.Bartel et al., contribution to the
1983 EPS Brighton Conference,

55) TASSO Collaboration, M.Althoff et al., DESY 83-064,

56) P.H.Damgaard, Nucl.Phys. B211 (1983) 435,

57) PLUTO Collaboration, contribution to the 1983 EPS Conference
in Brighton,

58) S.J.Brodsky and G.P.Lepage, Phys.Rev. D 24 (1981) 1808,

59) C.Peterson, T.F.Walsh and P.M.Zerwas,
Nucl.Phys. B 174 (1980) 424,

60) E.Witten, Nucl.Phys. B 120 (1977) 189,
W.R.Frazer and J.F.Gunion, Phys.REv. D 20 (1979) 147
C.H.Llewellyn Smith, Phys.Lett. 79B (1978) 83,
R.Dewitt et al., Phys.Rev. D 19 (1979) 166,

61) PLUTO Collaboration, Review talk by W.Wagner at the Int.
Workshop on Photon-Photon Collisions,
Aachen, April 1983 (PITHA 83/17)

62) Review by M.Pohl, DESY 83-047,

63) Double equivalent photon approximation A.Coureau CAL 82/19 (1982)

64) W.A.Bardeen and A.J.Buras, Phys.Rev. D 20 (1979) 166,
D.W.Duke and J.F.Owens, Phys.Rev. D 22 (1980) 2280,
T.Vematsu and T.F.Walsh, Fermilab-PUB-81/55-THY

65) JADE Collaboration, W.Bartel et al., Contribution to the
1983 EPS Conference in Brigthon, see also DESY 82-064,

66) CELLO Collaboration, H.-J.Behrend et al., DESY 83-018;
Phys.Lett. 126 B (1983) 391.